MODELING INTERFERENCE IN UNIFORMLY RANDOM WIRELESS NETWORKS: THEORY AND APPLICATIONS

A Thesis

Submitted to the Graduate School
of the University of Notre Dame
in Partial Fulfillment of the Requirements
for the Degree of

Master of Science
in
Electrical Engineering

by

Sunil Srinivasa, B. Tech

Martin Haenggi, Director

Graduate Program in Electrical Engineering
Notre Dame, Indiana
December 2007

MODELING INTERFERENCE IN UNIFORMLY RANDOM WIRELESS NETWORKS: THEORY AND APPLICATIONS

Abstract

by

Sunil Srinivasa

This thesis deals with the modeling of interference in a uniformly random wireless network with fading. The channel access mechanism considered is slotted ALOHA, and to obtain a fairly general set of results, the channel fading amplitude is taken to be Nakagami-m distributed. Under these settings, we obtain a closed-form expression for the moment generating function (MGF) of the interference power. The MGF is used to compute the interference moments, which accurately depict the asymptotic behavior of the network interference as the number of nodes increases. An important application of the interference characterization is the evaluation of the system outage performance.

As another application, we study the problem of path loss exponent (PLE) estimation in large wireless networks, which is relevant to several important topics in communications such as localization, energy-efficient transmission and handoff initiation in cellular networks. We formulate three different algorithms for PLE estimation, each based on a specific network characteristic. We also provide simulation results to demonstrate the performance of the algorithms and quantify the estimation errors.

To my parents and brother

for their love, support and encouragement

CONTENTS

FIGURES

TABLES

ACKNOWLEDGMENTS

There are a number of people I wish to thank for making my experience as a graduate student one of the most rewarding periods of my life. First off, I would like to thank my advisor Dr. Martin Haenggi for his continual support and guidance over the past two years. His seemingly boundless energy, encouragement, and loyalty to students has been truly inspirational. Dr. Haenggi always showed great faith in my abilities and allowed me to work independently, but at the same time provided invaluable advice at the necessary times. Without his support and guidance, this work could not have been accomplished. I would also like to thank Dr. Thomas Fuja and Dr. Panos Antsaklis for having found some time out of their busy schedule and willing to be on the committee for my Masters defense.

I am extremely grateful to all my friends at Notre Dame for making my stay here a memorable one. Special thanks to my group-mates Radha Krishna Ganti, Min Xie and Daniele Puccinelli for providing feedback on my work and offering ideas, comments and suggestions from time to time. I also thank several colleagues - Maiya, Shyam, Mallu, Krishnan, Sai, Su, Badri to name a few - for all the good times that we had.

Finally, I shall forever be grateful to my parents and brother. Needless to say, this work could not have been completed without their constant love, support and encouragement. Also, thanks to Skype^{TM}, I never really felt "away" from home!

CHAPTER 1

INTRODUCTION

> **Interference**: A coherent emission having a relatively narrow spectral content, e.g., a radio emission from another transmitter at approximately the same frequency, or having a harmonic frequency approximately the same as another emission of interest to a given recipient, and which impedes reception of the desired signal by the intended recipient.
>
> - Federal Standard 1037C: Glossary of Telecommunication Terms

1.1 Interference in Wireless Networks

A wireless ad hoc or sensor network is typically formed by randomly deployed motes that possess self-organizing capabilities [1]. Due to the stringent energy constraint on these devices, a natural communication strategy to conserve battery life is to reduce the range of transmission and employ multihop routing, where relays assist in the delivery of packets from the sources to the destinations. Owing to transmissions across several transceiver pairs, interference is commonly experienced in such systems. The interference can be between transmitters communicating with a common receiver (e.g., many motes sending data to a base station or a fusion center (uplink)), between signals from a single transmitter to multiple receivers (e.g., downlink), or between different transmitter-receiver pairs (e.g., interference between many nodes communicating with several base stations). It is often argued that the performance of wireless systems is limited by interference more than by any other single effect.

Despite the increasing focus on the analysis of ad hoc and sensor networks in recent years, the effect of interference in such systems has not been studied extensively. The primary reason for this is that it is often intractable to model the interference accurately. Particularly, in a network where nodes are distributed randomly, there might not exist a closed-form expression for the distribution of the interference. Even if the interference in the system can be explicitly specified, it might make further analysis intractable and thus not provide much insight on important quantities such as the signal-to-interference ratio (SINR), routing energy consumption, throughput, or end-to-end delay.

1.2 Combating Interference

Due to the above reasons, the inclusion of interference in analyses is often circumvented by assuming one of the following simplified channel models.

1) It is sometimes assumed that the noise power is much larger than the interference power, so that the SINR is equivalent to the signal-to-noise ratio (SNR). In other words, thermal noise swamps the interference, which can thus be neglected in analyses.

2) Interference is usually tackled by employing various multiplexing techniques, of which the major ones are:

a) Time division multiple access (TDMA) makes use of multiple time slots. The system is assumed to have a perfect MAC scheme that intelligently schedules the transmissions. Each user is assigned a separate time slot during which it exclusively uses the medium while all others wait.

b) Frequency division multiple access (FDMA) is a scheme where users share the radio spectrum. It divides the frequency band into segments and assigns to each user one of these sub-channels.

c) Code division multiple access (CDMA) is a technique where users are separated by codes. All users share all the time-frequency degrees of freedom. Users' data are spread (and despread) using a family of orthogonal codes.
d) Space division multiple access (SDMA) divides space to gain more channels. Using smart antenna technology, spatial signal signatures such as the direction of arrival (DOA) of the signal are calculated, and used to track and locate the antenna beam on the mobile/target. With the location of the mobile user known, the radiation pattern of the antenna is set to obtain the highest gain in that direction and reduce interference to other users.

3) The interfering nodes are assumed to be far from the transceiver pair so that the interference due to them may be neglected. Alternatively, the signal power can be considered to be high relative to the interference or the traffic in the system may be assumed to be light.

4) In multi-user systems, the effect of multiple-access interference is handled by using interference cancellation techniques. These methods basically decode the desired information and use this knowledge to subtract out interference successively from the received signals at the other receivers. Thus, signal processing is used after detection to reduce the influence of interference on future decisions. Though simple and robust, this technique is decidedly suboptimal particularly when the number of interferers is large.

1.3 Related Work

We now provide a brief overview of prior work that has dealt with interference in wireless networks. A commonly considered system is the infinite random network where nodes are distributed as a homogeneous Poisson point process (PPP). The analogy between interference in such networks and stable distributions (described

later) is observed in [2], [3]. Also, for Poisson networks, the throughput and outage performances are well-studied [3]-[7] under different system models and channel parameters. [8] focuses on the medium access control of large mobile, multihop wireless networks and analyzes various optimization problems concerned with the spatial density of progress of packets. [9] defines and studies the transmission capacity of wireless ad hoc networks in the presence of interference.

There also exists a body of literature on systems with regular topologies. In [7], the authors derive the distribution of the interference power for fading networks, where nodes are located on a lattice. The throughput of regular networks is studied in [10]-[12]. [13] derives some properties of interference in ad hoc networks where nodes form a planar Poisson clustered process and provides bounds on the outage probability and transmission capacity.

1.4 Organization and Main Contributions of the Thesis

Owing to the mathematical complexity involved, analytical results on the distribution of the interference exist only for a few particular classes of networks. In this work, we study a new type of network for which the interference in the system can be analytically studied and expressed in a closed form. Specifically, we characterize the interference in a finite uniformly random network where nodes contend for the channel via the slotted ALOHA mechanism. Applications include evaluating the network outage performance and estimating the path loss exponent of the channel, based on the interference characteristics.

The organization of this work is as follows. The thesis is divided into two distinct, yet related parts. The first part deals with the theory of modeling interference in uniformly random networks and derives some important analytical results. The subsequent part deals with applications of the first part and primarily tackles the

problem of path loss exponent estimation in large networks. Our main contributions are the following.

1) Though the spatial arrangement of nodes in a network is often taken to be a PPP in analyses, this assumption is impractical particularly when the number of nodes is small. Chapter 2 considers a new type of network that we call the "binomial" network, where a fixed number of N nodes are uniformly randomly distributed in a d-dimensional ball of radius R. Transmitters access the channel via the slotted ALOHA mechanism with a certain contention probability, and to obtain a fairly general set of results, the channel fading amplitude is taken to be Nakagami-m distributed. In this chapter, we primarily derive some analytic results for the interference power observed at the center of the ball. Specifically, we obtain a closed-form expression for the moment generating function (MGF) of the interference power. This is used to compute the interference moments and to evaluate the network outage performance. The moments provide an accurate characterization of the asymptotic behavior of the network interference as the number of nodes increases. By transforming the binomial network to the Poisson network, we model the interference in the latter system.

2) The second part of the thesis (Chapter 3) addresses the problem of estimating the path loss exponent (PLE) in large wireless networks, which is relevant to several important topics in communications such as localization, energy-efficient transmission and handoff initiation in cellular networks. Though analyses in many problems assume that the value of the PLE is known a priori, it is often not the case, and an accurate estimate is crucial for the study and design of systems. In this chapter, we study the estimation problem for a large wireless network where nodes are distributed as a PPP on the plane. We consider the channel amplitude to be Nakagami-m distributed and the MAC scheme to be slotted ALOHA. Under

these settings, our work focuses on three separate algorithms for path loss exponent estimation based on results from the prior part. Simulation results are provided to demonstrate the performance of the algorithms and quantify the estimation errors.

CHAPTER 2

MODELING INTERFERENCE IN UNIFORMLY RANDOM WIRELESS NETWORKS

2.1 Introduction and Motivation

In most cases in literature, the distribution of nodes in a wireless network with randomly scattered nodes is taken to be a homogeneous PPP, since the study of such a system is analytically convenient and leads to some insightful results. For the so-called "Poisson network" of intensity λ, the number of nodes $\Phi(V)$ in any given Borel set of Lebesgue measure V is Poisson with mean λV. Accordingly,

$$\Pr(\Phi(V) = k) = \exp(-\lambda V)\frac{(\lambda V)^k}{k!}.$$

As a consequence, the number of nodes in disjoint sets are independent of each other [14]. A homogeneous PPP is both stationary and isotropic. Even though practical networks may be created by dropping nodes uniformly randomly, they differ from Poisson networks in certain aspects. First, networks are usually formed by scattering a fixed (and finite) number of nodes in a given area (or very close to it). The underlying nodal distribution forms a *binomial point process* (BPP), which we describe later. Secondly, the point process formed is generally non-stationary and non-isotropic, meaning that the network characteristics as seen from a node's perspective is not homogeneous for all nodes. Intuitively, nodes near the boundary are

less susceptible to interference than the ones in the center. Furthermore, the number of nodes in disjoint sets are not independent but governed by the multinomial distribution. Fig. 2.1 shows a realization of the two processes with the same density. The PPP is clearly not a good model at times; there may be more points in the realization than the number dropped. A simple scenario where the PPP assumption is not suitable is when we have a network with a small number of nodes. Besides, the operation of protocols may be relying on a certain number of nodes being present in the network. This motivates the need to study and accurately characterize finite uniformly random networks, in an attempt to extend the plethora of results for the PPP to the often more realistic case of the BPP. We call this new model a "binomial network".

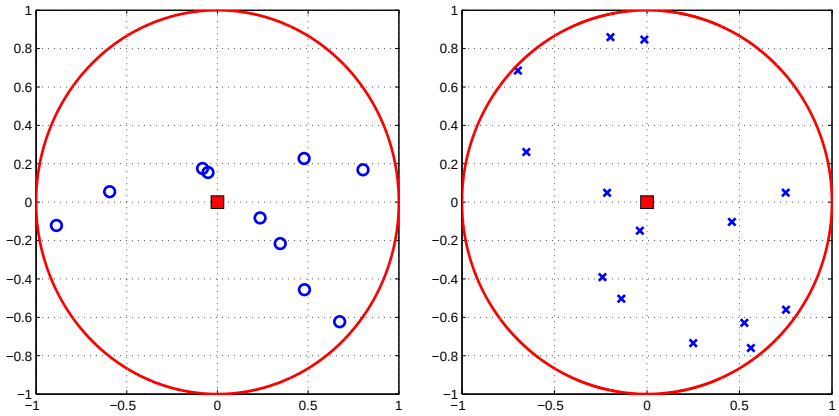

Figure 2.1. (Left) A realization of 10 nodes uniformly randomly distributed in a circular area of unit radius. (Right) A particular realization of the Poisson network with the same density (λ =3.18) has 14 nodes. The shaded box at the origin represents the base station.

A typical binomial network consists of several nodes transmitting to a central base station that collects data. During communication, these nodes potentially in-

terfere with each other. In order to accurately determine network parameters such as outage, throughput or transmission capacity [9], the interference distribution needs to be calculated. However, the pdf of the interference can be evaluated in closed-form only for a very small number of cases. We work around this issue by resorting to moment generating functions. In this thesis, the MGF of the interference at the origin is analytically obtained and used to compute the cumulants of the interference for a wide range of path loss exponents. The moments of the interference are used to give a rough idea of when the interference actually converges to a Gaussian distribution as the number of nodes in the network is increased. For cases where the central limit theorem is valid, the kurtosis of the interference is used to determine the rate of convergence to the Gaussian. We also show that the singularity of the interference due to nodes close to the origin is removed by employing a modified path loss model or having a guard zone around the receiver. Other applications of the MGF include estimating the network outage performance.

The binomial point process: A d-dimensional BPP is formed as a result of distributing N points independently uniformly and in a compact set $W \subset \mathbb{R}^d$. For a Borel subset V of W, the number of points in V is binomial(n, p) with parameters $n = N$ and $p = \nu_d(A)/\nu_d(W)$, where $\nu_d()$ is the standard d-dimensional Lebesgue measure. Accordingly,

$$\Pr(\Phi(V) = k) = \binom{n}{k} p^k (1-p)^{n-k}.$$

The intensity of this process is defined to be $N/\nu_d(W)$. Conditioned on the total number of nodes in a given volume, the PPP transforms into the BPP [14].

2.2 System and Channel Model

There are a total of N nodes uniformly randomly distributed in a d-dimensional ball of radius R centered at the origin, denoted as $b_d(0, R)$. The density of the

process is given by $\lambda = N/(c_d R^d)$, where $c_d = \nu_d(b_d(0,1))$. c_d can be expressed in terms of the gamma function as

$$c_d = \frac{\pi^{d/2}}{\Gamma(1+d/2)}.$$

We assume that each transmitting node collects data and sends it to a base station positioned at the origin. The channel access scheme is taken to be slotted ALOHA with contention probability p. Fig. 2.2 depicts the system model for the two-dimensional case. There are a total of N nodes and the ones that are transmitting are shaded.

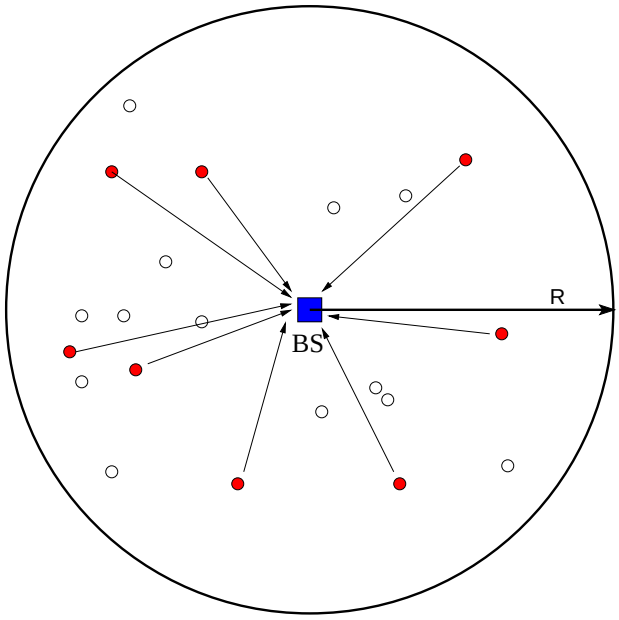

Figure 2.2. The system model for the 2-dimensional case.

The attenuation in the channel is modeled as a product of a distance component (that varies according to the large-scale path loss law with exponent γ) and a flat block fading component. In order to accommodate a variety of cases (including the one with no fading), the amplitude fading random variable H is assumed to be

Nakagami-m-distributed [15]. The functional form of the Nakagami-m distribution is

$$P_H(h) = \frac{2m^m}{\Gamma(m)\Omega^m} h^{2m-1} \exp\left(\frac{-m}{\Omega} h^2\right),$$

where the parameters $\Omega = \mathbb{E}[H^2]$ and $m \geq 1/2$. The Rayleigh fading case is realized by setting $m = 1$, and $m \to \infty$ is used to study the case of no fading. When dealing with received signal powers, we use the power fading variable denoted by $G = H^2$. Without loss of generality, we take the mean of G to be $\Omega = 1$. So, for $m = 1$, G is exponentially distributed with unit mean.

An outage is defined to occur when the SINR at the base station is smaller than a predefined threshold, Θ, which depends on the detector structure and the modulation and coding scheme [16]. Finally, we remark that the results presented in this work are for an "average network", that is one obtained by averaging over all possible realizations.

2.3 Interference Modeling

In this section, we first introduce the concept of *shot noise*. Using a variant of shot noise, the interference at the origin of a network where nodes are distributed as a BPP can be modeled. Employing this framework, we analytically derive the MGF of the interference which is extensively needed in the later sections of this chapter to derive the interference moments and the outage probabilities.

2.3.1 Shot Noise

The classical 1D shot noise is generated by the excitation of a memoryless, linear filter by a train of impulses whose arrivals form a homogeneous Poisson process [17] (see Fig. 2.3). The filter's impulse response $f(t)$ can assume different shapes such as a triangle, rectangle, exponential or a decaying power law. More generally, it

may be chosen out of a family of functions $f(g,t)$, where the g's are drawn from a certain probability distribution and the arrival times t's are Poisson with rate λ. The shot noise amplitude is given by

$$I(t) = \sum_j f(g_j, t - t_j). \tag{2.1}$$

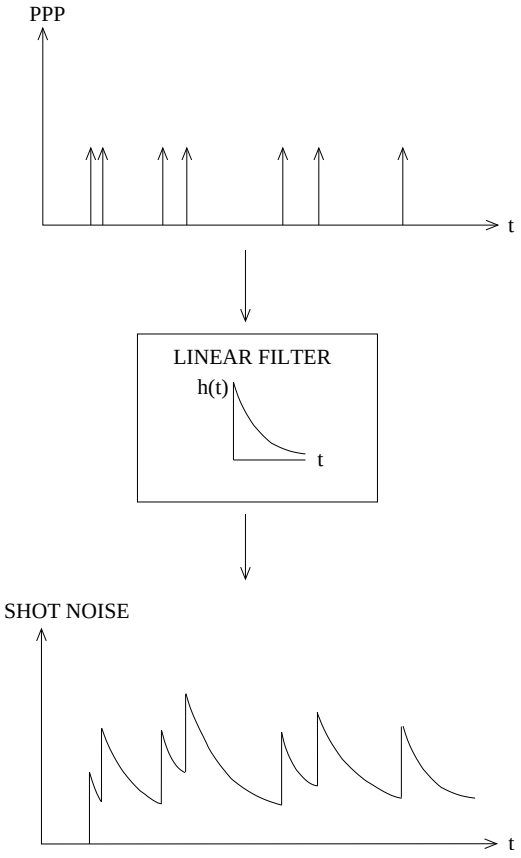

Figure 2.3. Shot Noise results from linearly filtering a PPP.

The arrival times $\{t_j\}$ are Poisson with rate λ and $\{g_j\}$ are independent identically distributed (i.i.d.) random variables and independent of t_j. All impulse functions $f(g,t)$ are assumed to be causal and integrable over $-\infty < t < \infty$ so that the series in (2.1) converges in distribution. As observed in [3], the shot noise process can be equivalently used for modeling interference in a 1D Poisson network

where the signal powers are decaying with distance according to a power law by replacing the arrival times with by the node locations.

Consider a modification of the 1D shot noise where the noise is produced by the excitation of a memoryless, linear filter by a train of impulses $i = 1, \ldots, N$ whose arrival times t_i's are drawn from a BPP. In other words, we condition on the total number of impulsive arrivals in shot noise (equal to N), while fixing the intensity of the process as λ. The amplitude of the resulting process is given by

$$I(g,t) = \sum_{i=1}^{N} f(g_i, t - t_i). \tag{2.2}$$

An analogy between the modified shot noise and the interference in a finite uniformly 1D random network can be drawn as follows. Consider the N interferers distributed as a BPP on the 1D interval $[0, N/\lambda]$, each transmitting at unit power to a base station located at the origin. Let the distance between node i and the base station be denoted by r_i and the fading state on the link between node i and the base station be g_i. Then the cumulative interference at the base station is

$$I(g,0) = \sum_{i=1}^{N} \frac{g_i}{r_i^{\gamma}}. \tag{2.3}$$

We see that if the impulse response of the filter in (2.2) is assumed to be the (non-causal) decaying power law (i.e. $f(g,t) = g\|t\|^{-\gamma}$), then the shot noise amplitude at time 0 is the same as the interference measured at the origin.

Extension of this framework to higher dimensional networks is straightforward. Intuitively, it can be thought of as projecting a d-dimensional process on to a 1D process with arrival times corresponding to the transmitting nodes' distances from the origin. Such a mapping procedure will not preserve the intensity of the original process, but nevertheless is a useful framework than can be employed to study the interference in binomial networks.

2.3.2 Stable Distributions

We now provide a short introduction to α-stable distributions, which we encounter in the later sections of this chapter.

Stable distributions approximate the distribution of normalizes sums of i.i.d. random variables making them useful in modeling the contribution of many small random effects [18]. They have been used to represent phenomena such as gravitational field of stars, temperature distributions in nuclear reactors, stresses in crystalline lattices, stock market prices and annual rainfall.

The stable distribution has the important property of stability, i.e., if a number of i.i.d. random variables have a stable distribution, then a linear combination of these variables will have the same distribution, except for possibly different shift and scale parameters. More formally, their definition is as follows.

Definition: A random variable X is said to have a stable distribution if it has a domain of attraction, i.e., for any $n \geq 2$, there is a sequence of i.i.d. random variables $X_1, X_2, \ldots, X_n$, a positive number R_n and a real number S_n such that

$$X_1 + X_2 + \ldots + X_n \stackrel{d}{=} R_n X + S_n,$$

where $X_1, X_2, \ldots, X_n$ are independent copies of X, and " $\stackrel{d}{=}$ " denotes equality in distribution. Stable distributions owe their importance in both theory and practice to a generalization of the central limit theorem.

A univariate stable distribution $S_\alpha(\sigma, \beta, \mu)$ is characterized by four parameters: the index of stability α, the scale parameter σ, the skewness parameter β and the shift parameter μ. The skewness parameter must lie in $[-1, 1]$, and when it is 0, the distribution is symmetric about μ. The scale parameter can take any non-negative real value, while $0 < \alpha \leq 2$, and $\mu \in \mathbb{R}$. A stable distribution can be equivalently defined via its characteristic function [18] as follows.

Definition: A random variable $X_\alpha(\sigma, \beta, \mu)$ is said to have a stable distribution (otherwise known as α-stable distribution) if its characteristic function has the following form:

$$\mathbb{E}[e^{i\omega X}] = \begin{cases} \exp\left(-\sigma^\alpha |\omega|^\alpha \left(1 - i\beta(\text{sign}(\omega)) \tan\frac{\pi\alpha}{2}\right) + i\mu\omega\right) & \text{if } \alpha \neq 1 \\ \exp\left(-\sigma|\omega|\left(1 + i\beta\frac{2}{\pi}(\text{sign}(\omega)) \ln|\omega|\right) + i\mu\omega\right) & \text{if } \alpha = 1. \end{cases}$$

Here, $i = \sqrt{-1}$ and $\text{sign}(\cdot)$ is the well-known sign function, with

$$\text{sign}(\omega) = \begin{cases} 1 & \text{if } \omega > 0, \\ 0 & \text{if } \omega = 0, \\ -1 & \text{if } \omega < 0. \end{cases}$$

The probability densities of α-stable distributions exist and are continuous but are known in closed form only for a few number of cases:

- The Gaussian distribution $S_2(\sigma, 0, \mu) = \mathcal{N}(\mu, 2\sigma^2)$, whose density is

$$\frac{1}{2\sigma\sqrt{\pi}} \exp(-(x-\mu)^2/4\sigma^2), \quad x \in \mathbb{R}.$$

- The Cauchy distribution $S_1(\sigma, 0, \mu)$, whose density is

$$\frac{\sigma}{\pi((x-\mu)^2) + \sigma^2}, \quad x \in \mathbb{R}.$$

- The Lévy distribution $S_{1/2}(\sigma, 1, \mu)$, whose density is

$$\left(\frac{\sigma}{2\pi}\right)^{1/2} \frac{1}{(x-\mu)^{3/2}} \exp\left(-\frac{\sigma}{2(x-\mu)}\right), \quad x \in (\mu, \infty).$$

Stable distributions with $\alpha < 2$ differ from Gaussian ones in many ways. First, the tails decay like a power function. The smaller α, the slower the decay, and the heavier the tails. Hence, they are likely to take values away from the median and exhibit larger fluctuations. These distributions always have infinite variance and when $\alpha \leq 1$, they have an infinite mean as well. Moreover, Gaussian distributions are always symmetric around their mean, whereas the other stable distributions

can exhibit arbitrary degrees of skewness. Thus, Gaussian distributions are not useful for modeling systems with high variability and random variables that are nonnegative, while other stable distributions are more flexible and do not exhibit such limitations.

2.3.3 Moment Generating Function

In this section, we adapt the shot noise model to model the interference in a binomial network. Using this framework, we analytically derive the MGF of the interference at the origin (base station) in closed-form. By transforming the BPP to a PPP, we also express the MGF of the interference in a Poisson network.

Theorem 1. *Consider a network consisting of N nodes uniformly randomly distributed in a d-dimensional ball of radius R. Let $\lambda = N/(c_d R^d)$. The channel access scheme is taken to be slotted ALOHA with parameter p. The MGF of the interference at the origin resulting only from the nodes in the annular region S with inner radius A and outer radius B $(0 \leq A < B \leq R)$ is*

$$M_I(s) = \left(1 - \frac{\lambda p}{N} \int_A^B \mathbb{E}_G \left[\left(1 - \exp\left(-sGr^{-\gamma}\right)\right) dc_d r^{d-1}\right] \mathrm{dr}\right)^N. \tag{2.4}$$

Proof: Let K denote the number of nodes in the region S. The probability distribution of K is by definition binomial,

$$P_K(k) = \binom{N}{k} \left(\frac{B^d - A^d}{R^d}\right)^k \left(1 - \frac{B^d - A^d}{R^d}\right)^{N-k}.$$

The interference at the origin due to the k nodes in the annulus is given as a sum of the received signal strengths from the individual nodes.

$$I(g, 0) = \sum_{i=1}^{k} I_i(g_i, r_i) = \sum_{i=1}^{k} t_i g_i r_i^{-\gamma}, \tag{2.5}$$

where the t_i's are independent realizations of the Bernoulli random variable T with $\Pr(T = 1) = p$ and $\Pr(T = 0) = 1 - p$. T is the random variable representing whether a node is transmitting or not.

The MGF of the interference $M(s) = \mathbb{E}\left[e^{-sI(g,0)}\right]$, where the expectation is taken over the fading states G, the variable T and the locations of the nodes[1]. As the I_i's are independent, the conditional MGF (given that there are k nodes) is expressible in a product form. We have

$$M_{I|k}(s) = \mathbb{E}\left[e^{-s(I_1(g_1,r_1)+I_2(g_2,r_2)+\ldots+I_k(g_k,r_k))}\right] = M_1(s)M_2(s)\cdots M_k(s). \quad (2.6)$$

Since the nodes are uniformly distributed in the annular volume, we have for each i, $1 \leq i \leq k$

$$M_i(s) = \frac{1}{c_d\left(B^d - A^d\right)} \int_A^B \mathbb{E}_G\left[dc_d r^{d-1}\left(1 - p + p \cdot \exp\left(-sGr^{-\gamma}\right)\right)\right] \mathrm{dr}. \quad (2.7)$$

All the interference terms are i.i.d., therefore each of the MGFs takes the same form, and we have

$$M_{I|k}(s) = \left(\frac{d}{B^d - A^d} \int_A^B \mathbb{E}_G\left[r^{d-1}\left(1 - p + p \cdot \exp\left(-sGr^{-\gamma}\right)\right)\right] \mathrm{dr}\right)^k. \quad (2.8)$$

Taking the inverse Laplace transform yields

$$P_{I|K}(x|k) = \frac{1}{2\pi} \int_{c-i\infty}^{c+i\infty} e^{sx} \left(\frac{d}{B^d - A^d} \int_A^B \mathbb{E}_G\left[r^{d-1}\left(1 - p + p \cdot e^{-sGr^{-\gamma}}\right)\right] \mathrm{dr}\right)^k \mathrm{ds},$$

where c is a real number appropriately chosen so that the contour path of integration is in the region of convergence of $M_I(s)$.

Using the law of total probability, we obtain

$$\begin{aligned} P_I(x) &= \sum_{k=0}^{N} \Pr(K = k) P_{I|K}(x|k) \\ &= \frac{1}{2\pi} \int_{c-i\infty}^{c+i\infty} e^{sx} \left(\frac{d}{R^d} \int_A^B \mathbb{E}_G\Big[r^{d-1}\left(1 - p + p \cdot \exp\left(-sGr^{-\gamma}\right)\right)\Big] \mathrm{dr} \right. \\ &\qquad \left. + 1 - \frac{B^d - A^d}{R^d}\right)^N \mathrm{ds}. \end{aligned}$$

[1]We use $\mathbb{E}\left[e^{-sI(\cdot)}\right]$ instead of $\mathbb{E}\left[e^{sI(\cdot)}\right]$, because we can obtain the pdf by simply taking the inverse Laplace transform of $M(s)$.

The MGF of the interference is thus given by

$$M_I(s) = \left(1 - \frac{p\left(B^d - A^d\right)}{R^d} + \frac{dp}{R^d}\int_A^B \mathbb{E}_G\left[r^{d-1}\left(\cdot \exp\left(-sGr^{-\gamma}\right)\right)\right]\mathrm{dr}\right)^N, \quad (2.9)$$

which is identical to (2.4). □

To simplify the expression for the MGF in (2.4), interchange the integral and expectation (per Fubini's theorem) to obtain

$$M_I(s) = \left(1 - \frac{\lambda p}{N}\mathbb{E}_G\underbrace{\left[\int_A^B \left(1 - \exp\left(-sGr^{-\gamma}\right)\right) dc_d r^{d-1}\mathrm{dr}\right]}_{D(s)}\right)^N. \quad (2.10)$$

$D(s)$ can be simplified as

$$\begin{aligned} D(s) &= c_d B^d\left[1 - e^{-sGB^{-\gamma}}\right] - c_d A^d\left[1 - e^{-sGA^{-\gamma}}\right] \\ &\quad + c_d\left(sG\right)^{d/\gamma}\Gamma\left(1 - d/\gamma, sGB^{-\gamma}\right) \\ &\quad - c_d\left(sG\right)^{d/\gamma}\Gamma\left(1 - d/\gamma, sGA^{-\gamma}\right), \end{aligned} \quad (2.11)$$

where $\Gamma(a, z)$ is the upper incomplete Gamma function[2] defined as

$$\Gamma(a, z) = \int_z^\infty \exp(-t)t^{a-1}\mathrm{dt}.$$

Eqn. (2.11) is obtained by a change of variables $t = sGr^{-\gamma}$ and integration by parts. The pdf of the interference is given by the inverse Laplace transform of the MGF.

Corollary 2. *The MGF of the interference seen at any node in a homogeneous Poisson network of density λ is*

$$M_{I(PPP)}(s) = \exp\left(-\lambda p\mathbb{E}_G\left[D(s)\right]\right). \quad (2.12)$$

Proof: If the number of nodes N tends to infinity in such a way that $\lambda = N/(c_d R^d)$ remains a constant, then the BPP asymptotically (as $R \to \infty$) behaves as a PPP [14]. Taking the limit as $N \to \infty$ in (2.10), we obtain (2.12). This is the MGF

[2]Mathematica: Gamma[a,z].

of the interference distribution as seen at the base station. Due to the stationarity of the Poisson process, this is representative of the MGF of the interference as seen at any node as well. The same expression for the practical cases of $d = 1$ and $d = 2$ is derived in [3]. □

2.4 Cumulants and Moments of the Interference

In this section, we use the MGF to analytically compute the moments of the interference distribution. These provide an indication of the interference's behavior. For example, they can be used to check if the interference converges to a Gaussian and if so, how fast. We work with cumulants rather than the moments since they are easier to obtain in this case. We are particularly interested in the first two cumulants which give the mean and variance respectively. The n^{th} cumulant of the interference is defined as

$$C_n = (-1)^n \frac{\mathrm{d}^n}{\mathrm{d}s^n} \ln M_I(s)\Big|_{s=0}. \tag{2.13}$$

Let

$$T_n := \begin{cases} \frac{dp}{R^d}\mathbb{E}_G\left[G^n\right]\left[\frac{B^{d-n\gamma}-A^{d-n\gamma}}{d-n\gamma}\right] & ,\gamma \neq \frac{d}{n} \\ \\ \frac{dp}{R^d}\mathbb{E}_G\left[G^n\right]\ln\left(\frac{B}{A}\right) & ,\gamma = \frac{d}{n}. \end{cases} \tag{2.14}$$

Proposition 3. *The cumulants can be expressed recursively as*

$$C_n = NT_n - \sum_{i=1}^{n-1} \binom{n-1}{i-1} C_i T_{n-i}. \tag{2.15}$$

Proof: The proof is very simple but tedious and as follows. One sees after repeatedly differentiating $D(s)$ that

$$\frac{\mathrm{d}^n}{\mathrm{d}s^n} D(s)\Big|_{s=0} = (-1)^{n+1}\frac{N}{\lambda p} T_n.$$

The details in the steps of differentiation are cumbersome and are omitted here. Denote the MGF of the interference (2.10) as $M_I^1(s)$ for the case of the exponent in $M_I(s)$ equal to one i.e.,

$$M_I^1(s) \;=\; 1 - \frac{\lambda p}{N}\mathbb{E}_G\left[D(s)\right]. \tag{2.16}$$

Then, the T_n's can also be expressed as

$$T_n = (-1)^n \frac{\mathrm{d}^n}{\mathrm{d}s^n} M_I^1(s)\Big|_{s=0}. \tag{2.17}$$

Therefore, if I^1 is the random variable whose MGF is $M_I^1(s)$, then the T_n's are the moments of I^1.

Now, the cumulants of $I(t)$ (2.13) are written as

$$C_n = N(-1)^n \frac{\mathrm{d}^n}{\mathrm{d}s^n} \ln M_I^1(s)\Big|_{s=0} = NC_n^1, \tag{2.18}$$

where C_n^1's are the cumulants of the variable I^1. By the recursive equation for the moment-cumulant relation [19], T_n and C_n^1 are related as

$$C_n^1 = T_n - \sum_{i=1}^{n-1} \binom{n-1}{i-1} C_i^1 T_{n-i},$$

whence (2.15) is obtained by taking $C_n^1 = C_n/N$. □

The mean and variance of the interference are easily calculated from the first two cumulants.

$$\mu_I = C_1 = \frac{Ndp}{R^d}\mathbb{E}_G\left[G\right]\left[\frac{B^{d-\gamma} - A^{d-\gamma}}{d-\gamma}\right], \tag{2.19}$$

and

$$\sigma_I^2 = C_2 = \frac{Ndp}{R^d}\mathbb{E}_G\left[G^2\right]\left[\frac{B^{d-2\gamma} - A^{d-2\gamma}}{d-2\gamma}\right] - \frac{\mu_I^2}{N}. \tag{2.20}$$

The mean and variance can also be computed using Campbell's theorem [14]:

$$\begin{aligned} \mu_I &= \mathbb{E}\left[\sum_{i=1}^{N} t_i g_i r_i^{-\gamma}\right] \\ &= \frac{Np}{c_d R^d}\mathbb{E}_G\left[G\right]\int_A^B \frac{dc_d r^{d-1}}{r^\gamma}\mathrm{d}r, \end{aligned} \tag{2.21}$$

and

$$\begin{aligned}
\sigma_I^2 &= \mathbb{E}\left[\left(\sum_{i=1}^{N} t_i g_i r_i^{-\gamma}\right)^2\right] - \mu_I^2 \\
&= \mathbb{E}\left[\sum_{i=1}^{N} t_i^2 g_i^2 r_i^{-2\gamma}\right] + 2\mathbb{E}\left[\sum_{\substack{i,j=1 \\ i<j}}^{N} t_i g_i r_i^{-\gamma} t_j g_j r_j^{-\gamma}\right] - \mu_I^2 \\
&= \frac{Np}{c_d R^d}\mathbb{E}_G\left[G^2\right]\int_A^B \frac{dc_d r^{d-1}}{r^{2\gamma}}\mathrm{d}r + 2\binom{N}{2}\left(\frac{\mu_I}{N}\right)^2 - \mu_I^2, \qquad (2.22)
\end{aligned}$$

which give the same value as (2.19) and (2.20) respectively.

The n^{th} moment μ_n is a n^{th} degree polynomial in the first n cumulants. The coefficients of the polynomial are those occurring in the Faà di-Bruno's formula [20]. For example, the first four moments are

$$\begin{aligned}
\mathbb{E}[I] &= C_1. \\
\mathbb{E}[I^2] &= C_2 + C_1^2. \\
\mathbb{E}[I^3] &= C_3 + 3C_1C_2 + C_1^3. \\
\mathbb{E}[I^4] &= C_4 + 4C_1C_3 + 3C_2^2 + 6C_1^2C_2 + C_1^4.
\end{aligned}$$

Under Nakagami-m fading, the cumulants (and moments) of the interference distribution can be exactly computed using the moments of the power fading variable G [15]:

$$\mathbb{E}_G[G^n] = \frac{\Gamma(m+n)}{m^n\Gamma(m)}. \qquad (2.23)$$

2.4.1 Cumulants for a Poisson Network

As we let $N \to \infty$ and $R \to \infty$ keeping the density λ constant, we arrive at a Poisson network. The n^{th} cumulant of I for a Poisson network is given by

$$C_n = \lambda p d c_d \mathbb{E}_G[G^n]\frac{B^{d-n\gamma} - A^{d-n\gamma}}{d-n\gamma}. \qquad (2.24)$$

When we let $B \to \infty$, a necessary condition for the n^{th} moment to be finite is $\gamma > nd$. We remark that for practical values of γ and d, this does not generally hold for $n > 2$, and thus all the higher-order cumulants are infinite.

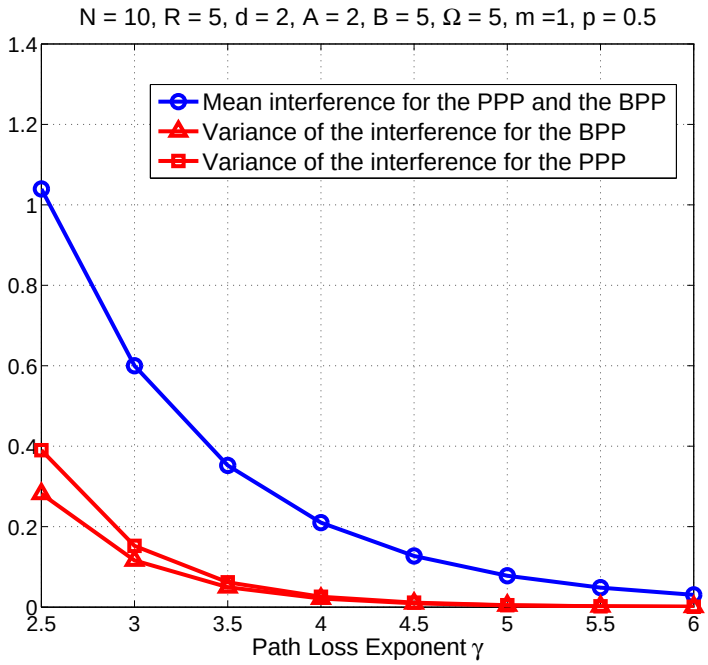

Figure 2.4. Comparison of the mean and variance of the interference for the BPP and PPP under Rayleigh fading.

Fig. 2.4 compares the mean and variance of the interference for the BPP and PPP system models versus the path loss exponent. Even though the mean interference is the same in both cases, the PPP network has a higher interference variance due to the uncertainty in the total number of nodes.

The ratio of the n^{th} cumulants with and without fading is given by

$$\frac{C_n|_{m=m}}{C_n|_{m=\infty}} = \frac{(m+n-1)!}{m^n(m-1)!} \tag{2.25}$$

Interestingly, the mean interference is independent of m, while the variance ratio

varies as is $1 + 1/m$. Thus the variance of the interference doubles for Rayleigh fading as compared to the no-fading case (as also observed in [4]).

2.4.2 Closed-form Interference Distributions

In this section, we investigate the behavior of the interference distribution under different values of the system parameters and study cases for which the interference pdf exists in closed form.

1) Stable Distribution :

For a Poisson network of density λ with $A = 0, B = \infty$ and $0 < d < \gamma$, the interference has an α-stable distribution with index of stability $\alpha = d/\gamma$ [18]. For the above parameters, the MGF takes the form

$$M_I(s) = \exp\left(-\lambda p c_d \mathbb{E}_G\left[G^{d/\gamma}\right]\Gamma\left(1 - d/\gamma\right) s^{d/\gamma}\right). \tag{2.26}$$

Since the sum of stable distributions is another stable distribution, the form of the interference distribution remains the same even when $\lambda \to \infty$.

Likewise, for a binomial network, the interference distribution approaches the α-stable form for $B < \infty$ as $N \to \infty$. As long as $d < \gamma$, the conditions for the central limit theorem are violated and the interference never converges to a Gaussian distribution. For the special case of $\alpha = 0.5$, the interference assumes the Lévy distribution and its pdf is obtained by taking the inverse Laplace transform as

$$P_I(x) = \sqrt{\frac{c}{\pi}} x^{-3/2} \exp(-c/x), \quad x \geq 0, \tag{2.27}$$

where $c = (\pi\lambda^2 p^2 c_d^2 \mathbb{E}_G^2[G^{1/2}])/4$. All the moments of the interference are infinite. Furthermore, the CDF can be written in terms of the Q-function as $F_I(x) = 2Q(\sqrt{c/x})$. The same expressions have been obtained earlier for the two-dimensional Poisson network for a deterministic channel [5] and in the presence of Rayleigh fading [6]. The Lévy distribution is plotted for different values of c in Fig. 2.5.

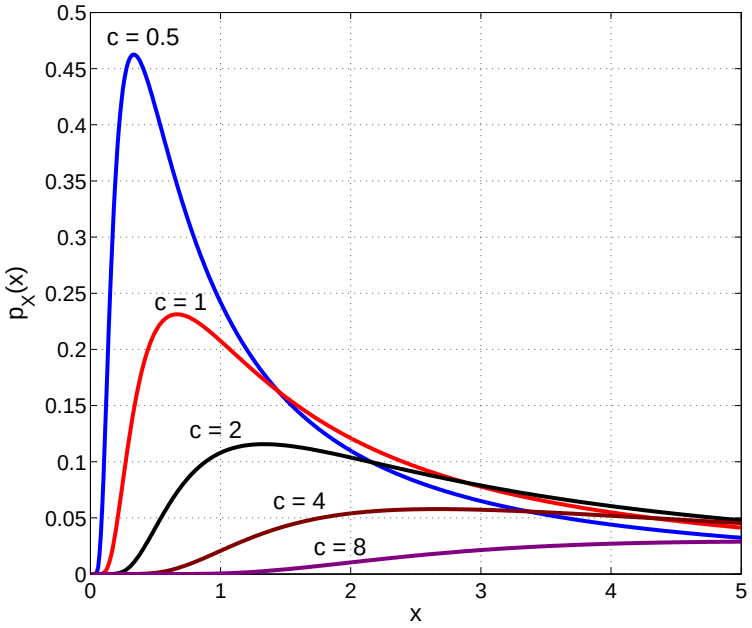

Figure 2.5. The Lévy distribution for various values of c.

2) Infinite with Probability 1 :

Under the conditions $A \geq 0, B = \infty, d \leq \gamma$, the interference will be infinite with probability one as $N \to \infty$. To show this, consider (2.10)

$$M_I(s) = \left(1 - \frac{\lambda p}{N}\mathbb{E}_G\left[D(s)\right]\right)^N.$$

For $B = \infty$, $d \leq \gamma$ and $s \neq 0$,

$$\begin{aligned} D(s) &= \frac{(sG)^{d/\gamma} dc_d}{\gamma} \int_0^{sgA^{-\gamma}} \frac{1 - \exp(-u)}{u^{1+d/\gamma}} \mathrm{d}u \\ &\geq \frac{(sG)^{d/\gamma} dc_d}{\gamma} \int_0^{c} \frac{1 - \exp(-u)}{u^{1+d/\gamma}} \mathrm{d}u \\ &\overset{(a)}{\geq} \frac{(sG)^{d/\gamma} dc_d (1 - \exp(-c))}{c\gamma} \int_0^{c} \frac{u}{u^{1+d/\gamma}} \mathrm{d}u \\ &\overset{(b)}{\geq} +\infty. \end{aligned} \tag{2.28}$$

where $c \in \mathbb{R}$ and satisfies $0 < c \leq sgA^{-\gamma}$. (a) holds since the function $(1 - \exp(-u))/u$ is monotonically decreasing with u. (b) is true since $d \leq \gamma$. Also, when $s = 0$, $D(s) = 1$. Therefore,

$$\lim_{N\to\infty} M_I(s) = \begin{cases} 1, & s = 0 \\ 0, & s \neq 0, \end{cases}$$

and hence,

$$\Pr(I < x) = 0 \quad \forall x \in [0, \infty). \tag{2.29}$$

3) Gaussian Distribution :

It is often assumed that the interference in a large random network is the sum of several i.i.d. contributions and is modeled as a Gaussian-distributed random variable. We now study cases where the interference is indeed Gaussian-distributed, and cases where it never converges to the Gaussian distribution.

a) $A > 0, B < \infty$:

If $C_n < \infty$ for $N = 1$ and $n = 1, 2$, then conditions for the central limit theorem are met and the interference approaches a Gaussian as the number of interferers N goes to ∞ [17].

For $A > 0$ and $B < \infty$ for any d and γ, all the moments are finite for $N = 1$, so in the limiting case,

$$P_I(x) \to \mathcal{N}(C_1, C_2) = \frac{1}{\sqrt{2\pi C_2}} \exp(-(x - C_1)^2/2C_2). \tag{2.30}$$

b) $A = 0, B < \infty$:

When $A = 0$, the interference approaches a Gaussian only for $d > 2\gamma$. For $1/2 \leq \gamma/d < 1$, the mean interference is finite for $N = 1$ while its variance is unbounded. Therefore, the interference never converges to a Gaussian as $N \to \infty$.

For $\gamma/d = 1$, all the moments of the interference are infinite, but the interference is not infinite with probability one.

c) $A > 0, B = \infty$:

In this case, the interference asymptotically approaches a Gaussian only for $d < \gamma$.

Table 2.1 summarizes the forms assumed by the interference distribution for various ranges of the system parameters.

TABLE 2.1

BEHAVIOR OF THE INTERFERENCE FOR VARIOUS RANGES OF THE PARAMETERS A, B, d AND γ

	$A > 0$, $B = \infty$	$A = 0$, $B = \infty$	$A = 0$, $B < \infty$	$A > 0$, $B < \infty$
$0 < \frac{\gamma}{d} < \frac{1}{2}$	$\Pr(I = \infty) = 1$ as $N \to \infty$	$\Pr(I = \infty) = 1$ as $N \to \infty$	$I \to$ Gaussian as $N \to \infty$	$I \to$ Gaussian as $N \to \infty$
$\frac{1}{2} \leq \frac{\gamma}{d} < 1$	$\Pr(I = \infty) = 1$ as $N \to \infty$	$\Pr(I = \infty) = 1$ as $N \to \infty$	$I \nrightarrow$ Gaussian as $N \to \infty$	$I \to$ Gaussian as $N \to \infty$
$\frac{\gamma}{d} = 1$	$\Pr(I = \infty) = 1$ as $N \to \infty$	$\Pr(I = \infty) = 1$ as $N \to \infty$	$I \nrightarrow$ Gaussian as $N \to \infty$	$I \to$ Gaussian as $N \to \infty$
$\frac{\gamma}{d} > 1$	$I \to$ Gaussian as $N \to \infty$	$I =$ α-stable for a PPP	$I \to$ α-stable as $N \to \infty$	$I \to$ Gaussian as $N \to \infty$

2.4.3 Kurtosis and Convergence to a Gaussian

In the case that C_n exists for $N = 1$ and $n = 1, 2$, it is known that the interference approaches a Gaussian distribution as $N \to \infty$. But how fast does this occur? The kurtosis is a good parameter to assess the rate of the process at which the distribution approximates a Gaussian. In probability theory, (excess) kurtosis is a measure of the "peakedness" of the probability distribution of a real-valued random

variable. Higher kurtosis means more of the variance is due to infrequent extreme deviations, as opposed to frequent modestly-sized deviations. It is commonly defined as the fourth central moment divided by the square of the variance of the probability distribution minus 3, i.e.,

$$\kappa(I) = \frac{\mathbb{E}\left[(I-\mu_I)^4\right]}{\sigma_I^4} - 3 = \frac{C_4}{C_2^2}. \tag{2.31}$$

The "-3" term is present to normalize the Gaussian distribution's (excess) kurtosis to zero.

Fig. 2.6 plots the kurtosis of the interference variable for various values of the network parameters and helps calculate the N for which its behavior is approximately Gaussian (kurtosis$\rightarrow 0$). In each case, the interference distribution converges to a Gaussian.

2.5 Eliminating the Singularity of the Interference at the Origin

In this section, we show that it is possible to eliminate the diverging moments of the interference by using either a modified path loss model or by employing a guard zone around the base station.

2.5.1 Modified Path Loss Model

The decaying path loss model does not make much sense for small distances as it claims that the signal strength is amplified for the case $r < 1$. In order to overcome this flaw, the path loss model is taken by some authors to be $(1+r)^{-\gamma}$ or $\min\{1, r^{-\gamma}\}$. In this subsection, we consider the latter path loss model. For $A = 0, B = R$ (assumed to be > 1), the total interference at the origin can be taken as the sum of two contributions I_1 and I_2, which are due to interferers from $b_d(0,1)$ and $b_d(0,1)^c$ respectively. The channel seen by the transmitting nodes in $b_d(0,1)$

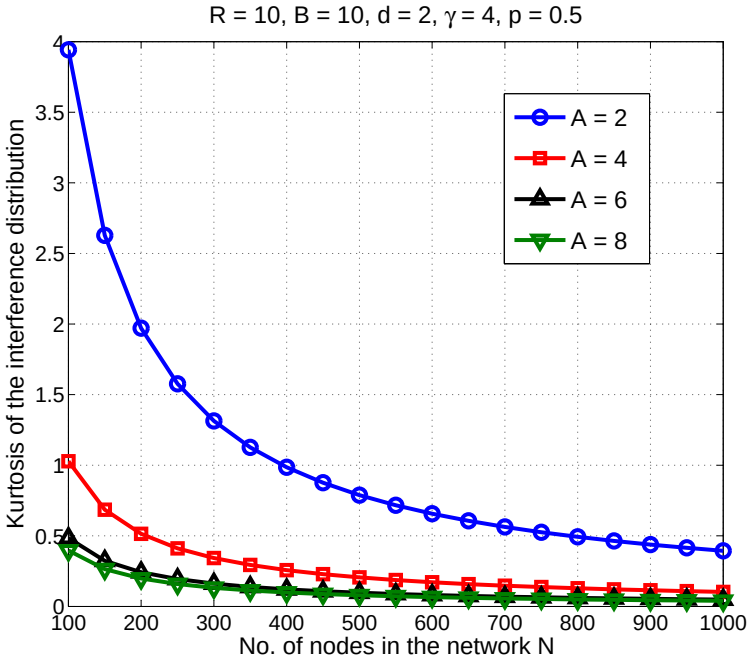

Figure 2.6. Kurtosis of the interference distribution for different values of the inner radius A.

has a path loss exponent $\gamma = 0$. The mean of I is therefore calculated to be

$$\mu_I = \frac{Ndp}{R^d}\left[\frac{1}{d} + \frac{R^{d-\gamma} - 1}{d - \gamma}\right] = \frac{Np}{R^d}\left[\frac{dR^{d-\gamma} - \gamma}{d - \gamma}\right].$$

The variance is harder to calculate since the interferences I_1 and I_2 are negatively correlated (because the total number of nodes is fixed).

2.5.2 Guard Zone

In wireless networks, it is necessary to suppress transmissions by nodes close to the desired receiver in order to achieve successful communication e.g. using CSMA. This exclusion zone around the receiver is known as the guard zone [21]. Not having a guard zone can result in undesirably high outage probabilities since the interference caused by the nearby transmitters is often very high. Assume that the base station

has a guard zone of radius d_0, in which nodes do not transmit. This way, all the moments are made finite and the MGF of the interference for this case can simply be calculated by putting $A = d_0$ in (2.10).

2.6 Outage Analysis

In this section, we determine the outage performance of the binomial network under Rayleigh fading. We assume that the background noise in the network is much weaker than the interference and neglect it in our analysis. Therefore, an outage occurs if the SIR at the receiver is less than a certain threshold Θ. The outage at the origin is calculated by assuming that the desired transmitter node is located at unit distance from the origin and is transmitting at unit power. The received signal power at the base station due to that node is therefore exponential with unit mean. The outage probability $\Pr(\mathcal{O})$ is calculated as

$$\begin{aligned} \Pr(\mathcal{O}) &= \mathbb{E}_I \left[\Pr(G < I\Theta \mid I)\right] \\ &= \mathbb{E}_I \left[1 - \exp(-I\Theta)\right] \\ &= 1 - M_I(\Theta). \end{aligned} \tag{2.32}$$

The probability of success p_s is equal to $M_I(\Theta)$.

Fig. 2.7 compares the success probabilities for the PPP and BPP nodal distributions. We see that the PPP model provides an upper bound on the performance in a binomial network and is not a good assumption to use when there are very few interferers in the network. This is also apparent from Jensen's inequality and the fact that $D(s)$ (see (2.11)) is concave w.r.t s.

2.7 Chapter Summary

In this chapter, we characterized the interference in a network where the nodes are distributed as a BPP. Using the shot noise framework, a closed-form analytical

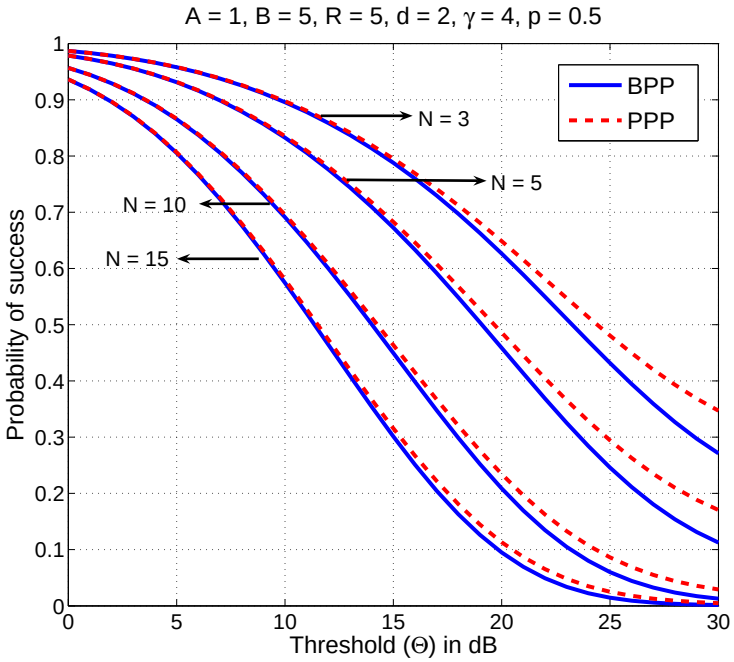

Figure 2.7. Comparison of success probabilities for Poisson and binomial networks for different values of N under Rayleigh fading.

expression for the MGF of the interference is obtained. The cumulants of the interference are calculated and used to study the asymptotic behavior of the interference as the number of transmitters is increased. For certain values of the system parameters, the pdf of the interference is shown to converge to a Gaussian distribution. We also studied the outage behavior of the network and conclude that using the Poisson network model in analyses provides an overly optimistic estimate of the network's performance when the number of interferers is small and the threshold Θ is high, i.e., for high-rate communication.

CHAPTER 3

PATH LOSS EXPONENT ESTIMATION IN LARGE NETWORKS

3.1 Introduction

The wireless channel presents a formidable challenge as a medium for reliable high-rate communication and places fundamental limitations on the performance of networks. It is responsible not only for the attenuation in the strength of the propagated signal but also causes spatial and temporal variations in this loss that are unpredictable due to user movement and changes in the environment. In order to capture all these effects, the path loss for RF signals is commonly represented as the product of a deterministic distance component (large-scale path loss) and a randomly-varying component (small-scale fading). The large-scale path loss model assumes that the received signal strength falls off with distance according to a power law, at a rate termed the PLE. Fading describes the fluctuations in the received signal strength due to the constructive and destructive addition of its multipath components. While variations due to path loss happen over large distances (hundreds of meters), variations due to multipath occur over much shorter distances, on the order of the RF wavelength. The large-scale path loss is the simplest model for signal propagation and also a major component considered during the analysis and design of communication systems [22]. An critical issue is to characterize the large-scale behavior of the channel and accurately estimate the PLE, based solely on received signal measurements.

This problem is not trivially solvable even for a single link due to the existence of multipath and background thermal noise. For large ad hoc and sensor networks, the problem is further complicated due to the following reasons: First, the achievable performance of a typical wireless network is not only vulnerable to noise and fading, but also to interference due to the presence of simultaneous transmitters. Dealing with fading and interference simultaneously is a major difficulty in the estimation problem. Moreover, the distances between nodes are subject to uncertainty. Often, the distribution of the underlying point process can be statistically determined, but precise locations of the nodes are harder to measure. In such cases, we will need to consider the fading and distance ambiguities jointly, i.e., define a spatial point process that incorporates both. In this chapter, we present three different methods to accurately estimate the channel's PLE for large wireless networks in the presence of fading, noise and interference, based on the received interference measurements. We also provide simulation results to depict the performance of the algorithms and study the estimation error. Additionally, we furnish some basic methods to infer the intensity of the Poisson process, while providing Crámer-Rao lower bounds on the mean squared error (MSE) wherever possible.

3.2 Motivation and Related Work

3.2.1 Motivation

In this section, we illustrate the importance of knowing the PLE for tackling various issues in communication. In general, since the channel model is primarily defined by the PLE, analysis and design of wireless networks naturally rely heavily on its estimates. Though it is assumed in many problems that the value of the PLE is known a priori, this is not true in practice, and an accurate estimate of the PLE is crucial for solving them.

The topic of PLE estimation is closely related to that of localization and can essentially be thought of as its complementary problem. In sensor networks, node localization is an integral component of network self-configuration. When bestowed with the ability to detect their positions, ad hoc deployed sensor nodes can support a rich set of geographically aware protocols and accurately report the regions of detected events. Detailed knowledge of the nodes' locations is also needed for performing energy-efficient routing in a decentralized fashion. An important class of localization algorithms are the ones based on RSS measurements [23, 24] that need accurate estimates of the PLE to perform well. Another fundamental issue in wireless sensor networks is the sensing problem that deals with how well and accurately a target area or a phenomenon can be monitored. Of importance in such applications are characteristics such as the coverage and the connectivity of the network, and studying these properties need accurate estimates of the PLE.

Many of the existing results on capacity scaling for large ad hoc networks strongly depend on the PLE as well. With γ being the PLE, the best known achievability result [25] states that capacity scales as $n^{2-\gamma/2}$ for $2 \leq \gamma < 3$ and as $\sqrt{n}$ for $\gamma \geq 3$. Depending on the value of the PLE, appropriate routing strategies (nearest-neighbor hopping or hierarchical cooperative) may be implemented to reach the maximally achievable scaling of the system throughput. A good knowledge of the PLE is also essential for designing simple line networks. [26] discusses capacity results for TDMA-based linear networks and shows that the optimum number of hops needed to achieve a desired end-to-end rate strongly depends on the PLE value. For example, when the desired (bandwidth-normalized) spectral efficiency exceeds the PLE, single-hop transmission outperforms multihopping.

Energy consumption in wireless networks is a crucial issue that needs to be addressed at all the layers of the communication system. [27] analyzes the energy

consumed for several routing strategies that employ hops of different lengths in a large network with uniformly randomly distributed nodes. Using the results therein, we demonstrate that a good knowledge of the PLE is necessary for efficient routing. Consider the following two simple schemes where communication is assumed to occur only in a sector ϕ around the source-destination axis.

1) Route hop by hop across n nearest neighbors from the source to destination in the sector ϕ.

2) Transmit directly to the n'th neighbor in the sector ϕ. Here, n' is chosen in a way that the expected progress is the same for both the schemes.

It is seen from [27] that the ratio of the consumed energies for the two schemes is

$$\frac{E_1}{E_2} = \frac{n^2\Gamma(1+\gamma/2)\Gamma(n')}{\Gamma(n'+\gamma/2)},$$

where $\Gamma(.)$ represents the Gamma function and $n' = \frac{\pi}{4}(n^2-1)+1$. This is independent of ϕ and is plotted in Fig. 3.1 for different values of n. From the curves, we see that the PLE plays an important role in determining the more energy-efficient routing strategy. When γ is low, scheme 2 consumes less energy while relaying is beneficial at high PLE values.

The performance of contention-based systems such as slotted ALOHA is very sensitive to the transmission probability p and hence the optimal operating point of the system has to be chosen. The value of the contention parameter is determined based on various motives such as maximizing the network throughput [3, Eqn. 20] or optimizing the spatial density of progress [8, Eqn. 5.6]. Fig. 3.2 plots the per-node throughput versus p in a system running the slotted ALOHA protocol. It is seen that the throughput also depends greatly on the PLE and depending on the estimate of γ, the optimal value of the contention probability can be chosen.

PLE estimation is also an integral component of the cellular phone location

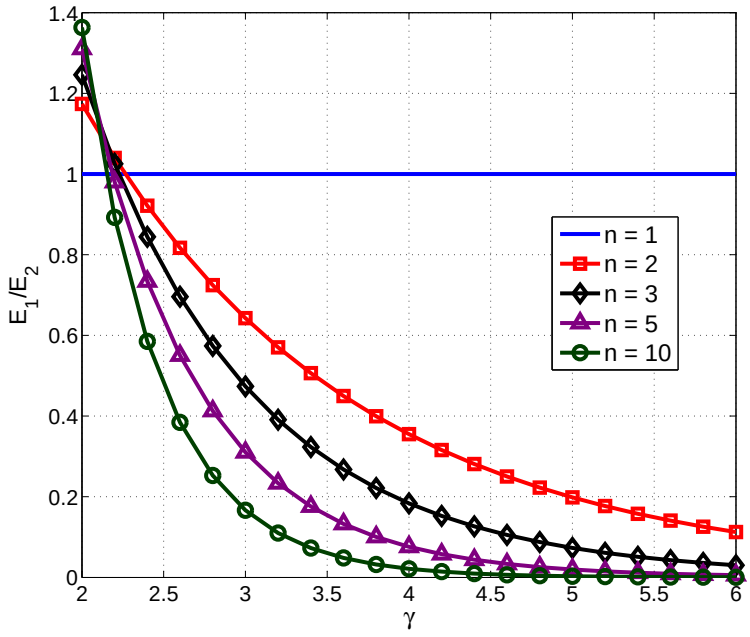

Figure 3.1. The ratio of the energies for the two schemes versus γ.

system, which has garnered considerable attention. There are several reasons why network providers need to estimate the position of mobile terminals in the network. Primarily, they have to be able to assist emergency communications, which needs accurate location estimates of the mobiles. Localization is also desired to provide positioning, tracking and navigation services to people with special needs, such as firefighters, soldiers, elderly patients, etc. Besides, knowing the PLE accurately helps determining when the handoff procedure needs to be initiated so that calls are not dropped. In addition, it helps carry out open loop power control efficiently.

3.2.2 Review of Literature

In this section, we survey some of the existing estimation methods in literature. Much of the past work on PLE prediction has focused on received signal

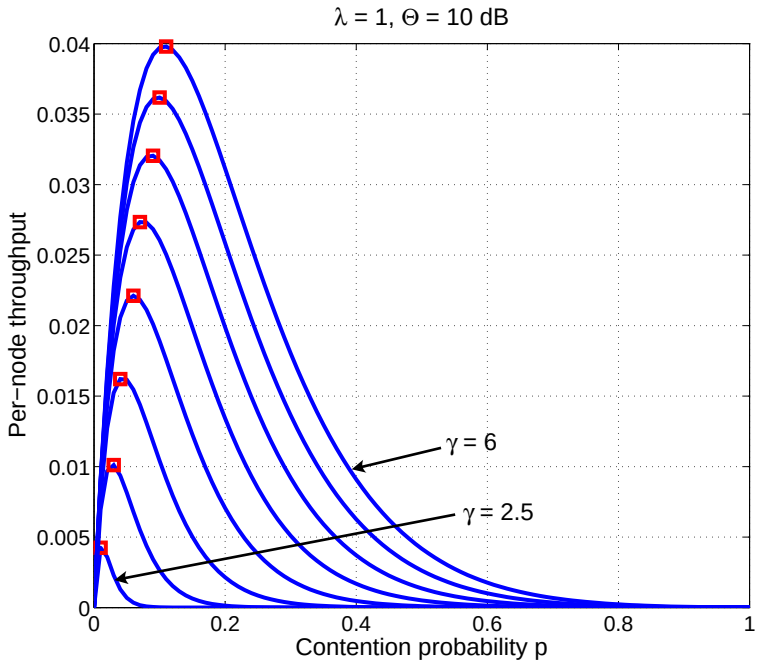

Figure 3.2. The per-node throughput for several values of γ. The optimal values of the contention parameter are marked as well.

strength (RSS)-based localization techniques. Most authors assume a simplified channel model consisting only of a large-scale path loss component and a shadowing counterpart, but we are not aware of any prior work that has considered fading and interference jointly in the system model.

1) Estimation based on a known internode distance probability distribution :

This is discussed in [28] and assumes that the distance distribution between two neighboring nodes i and j is known or can be determined easily. It also makes the simplified assumption that there is no interference in the system so that when i transmits, j's received signal is only due to node i. With the transmit power equal to P_0[dBm] (assume this is a constant for all nodes), the RSS at node j is modeled

by a log-normal behavior as

$$P_{ij}[\text{dBm}] \sim \mathcal{N}(\overline{P}_{ij}[\text{dBm}], \sigma^2_{\text{dB}}),$$

where σ denotes the log-normal spread and $\overline{P}_{ij}[\text{dBm}] = P_0[\text{dBm}] - 10\gamma \log_{10} d_{ij}$. Now, if the neighbor's distance distribution is given by $p_R(r)$, then

$$\overline{P}_{ij} = P_0 \mathbb{E}_R \left[R^{-\gamma} \right]. \tag{3.1}$$

E.g., if the internodal distance distribution is Rayleigh[1] with mean $\sqrt{\pi/2}$, then

$$\overline{P}_{ij} = P_0 2^{-\gamma/2} \Gamma(1 - \gamma/2). \tag{3.2}$$

The value of γ is obtained by equating $\overline{P}_{ij}$ to the empirical mean value of the received powers taken over several node pairs i and j. For the example stated above, the value of γ may be predicted using a look-up table.

2) Estimation based on a known, yet complex neighbor distance probability distribution :

If the nearest neighbor distribution is in a complicated form that is not integrable, an idea similar to the quantile-quantile plot can be used [28]. The quantile-quantile plot is a graphical technique for determining if two sets of data are drawn from a common distribution. Choose a set of N random points $\lambda_1, \lambda_2, \ldots, \lambda_N$ uniformly distributed in [0,1]. The quantile points of the nearest neighbor distance distribution $d_1, d_2, \ldots, d_N$ and the measured received power $p_1, p_2, \ldots, p_N$ corresponding to $\lambda_1 \ldots \lambda_N$ can be determined by setting

$$\Pr(D \geq d_i) = \lambda_i \text{ and } \Pr(P \geq p_i) = \lambda_i, \quad i = 1, 2, \ldots, N,$$

[1]The nearest neighbor distance function when the nodal arrangement is a planar PPP is Rayleigh distributed. The mean value assumed is just for the sake of convenience.

where d denotes the (known) neighbor distance distribution and P, the distribution of the received power. An estimation of γ can be obtained by minimizing the MSE

$$\text{MSE}(\gamma) = \sum_{i=1}^{N} (p_i - P_o d_i^{-\gamma})^2. \tag{3.3}$$

Writing out the power terms in dBm, we get an equivalent MSE term,

$$\text{MSE}(\gamma) = \sum_{i=1}^{N} (p_i[\text{dBm}] - P_o[\text{dBm}] + 10\gamma \log_{10}(d_i))^2.$$

Differentiating the above expression and setting it to zero yields the estimate

$$\hat{\gamma} = \frac{-\sum_{i=1}^{N} (p_i[\text{dBm}] - P_o[\text{dBm}]) \log_{10}(d_i)}{\sum_{i=1}^{N} 10(\log_{10}(d_i))^2}. \tag{3.4}$$

3) Estimation that does not rely on distance measurements :

Sometimes, it might not be possible to obtain the neighbor distance distribution. The idea of estimating γ using the concept of the Cayley-Menger determinant [28] is useful in such cases. For this method to work, a set of fully connected quadrilaterals in the network need to identified. By fully connected quadrilaterals, we mean a set of four nodes located such that the received power from any node to any other is above a certain threshold level. For obvious reasons, such a method fails when fading is considered. With these four nodes, one can have six unique tuples of the measured power and distances ($p_{ij}.d_{ij}$). [28] uses the idea that for a two-dimensional network, the Cayley-Menger matrix can have rank at most equal to 3. Equating the Cayley-Menger determinant to zero is used to estimate the value of γ. However, the value of γ estimated as above is shown to have a large bias. The pattern matching method works to remove this bias.

4) Pattern Matching Technique :

[28] observes that that the relationship between $\mathbb{E}(\hat{\gamma})$, σ and γ is independent of the distribution of the vertices of various quadrilaterals as well the shape of

the network. They use a pattern matching technique to estimate the PLE with the knowledge of the received power amplitude alone. Their numerical evaluation shows that the bias of γ has an approximate linear relationship with σ for a fixed γ. A look-up table is generated and is used in the estimation process to remove the bias that exists when using the principle of the Cayley-Menger determinant.

As described in the introduction, the situation is completely different when interference and fading are accounted for and we cannot use the commonly known RSS-based estimators directly.

3.3 System Model

We consider a large planar ad hoc network, where nodes are distributed as a homogeneous PPP Φ of intensity λ (assumed unknown). The PPP model for the nodal distribution is a ubiquitously used one and may be justified by claiming that sensor nodes are dropped from an aircraft in large numbers; for mobile ad hoc networks, it may be argued that terminals move independently of each other.

The attenuation in the channel is modeled as a product of the large-scale path loss with exponent γ and a flat block-fading component. To obtain a concrete set of results, the amplitude H is taken to be Nakagami-m distributed with parameter Ω. Letting $m = 1$ results in the well-known case of Rayleigh fading, while lower and higher values of m signify stronger and weaker fading scenarios respectively. The block fading assumption is necessary for our analysis and may be justified by assuming that the nodes or surrounding objects move slightly so that in each transmission block, different fading realizations are observed. When dealing with received signal powers, we use the power fading variable denoted by $G = H^2$. Useful in the later sections are the moments of G [15],

$$\mathbb{E}_G[G^n] = \frac{\Gamma(m+n)}{m^n \Gamma(m)} \Omega^n.$$

Note that $\mathbb{E}_G(G) = \Omega$ and is independent of m, while its variance is $\sigma_G^2(G) = \Omega^2/m$. Without loss of generality, we take $\Omega = 1$.

Since the PLE estimation is usually performed during network initialization, it is fair to assume that the transmissions in the system during this phase are uncoordinated. Therefore, we take the channel access scheme to be slotted ALOHA. We denote the ALOHA contention probability by a constant p. Consequently, the set of transmitters forms a PPP Φ' of intensity λp. Also, we assume that all the transmit powers are equal to unity. Then, the interference at receiving node y on the plane is given by

$$I_\Phi(y) = \sum_{z \in \Phi'} g_{zy} \|z - y\|^{-\gamma},$$

where g_{zy} is the fading gain of the channel and $\|\cdot\|$ denotes the Euclidean distance.

By definition, an outage occurs if and only if

$$\frac{g_{xy}\|x - y\|^{-\gamma}}{N_0 + I_{\Phi\setminus\{x\}}(y)} < \Theta, \tag{3.5}$$

where $I_{\Phi\setminus\{x\}}(y)$ denotes the interference in the network at y due to all the transmitters, except the desired one at x, and N_0 is the noise power.

3.4 Estimation of the density of the Poisson network

First, we furnish some basic methods to estimate the intensity of the network, which will be useful in the later sections of this chapter for estimating the parameters p and m. We also analyze Crámer-Rao lower bounds on the MSE wherever possible.

3.4.1 The Naive Solution

The most fundamental method to estimate the network's intensity is simply to use its definition. Observing the process through a 2D-window W, an unbiased estimator for the intensity is given by

$$\hat{\lambda} = \Phi(W)/\nu_2(W). \tag{3.6}$$

We know that $\Phi(W)$ is Poisson-distributed with mean $\lambda\nu_2(W)$ i.e., it is governed by a probability mass function

$$f(\Phi(W) = k; \lambda) = \exp(-\lambda\nu_2(W))\frac{(\lambda\nu_2(W))^k}{k!}. \tag{3.7}$$

The regularity condition is met in this case [29]

$$\frac{\partial}{\partial\lambda}\ln f(\Phi(W) = k; \lambda) = \frac{\nu_2(W)}{\lambda}\left[\hat{\lambda} - \lambda\right], \tag{3.8}$$

and thus, this is an efficient estimator meeting the following Crámer-Rao lower bound (CRLB) on the error variance.

$$\mathrm{MSE}(\hat{\lambda}) = \lambda/\nu_2(W). \tag{3.9}$$

Since Φ is ergodic, $\hat{\lambda}$ is strongly consistent in the sense that it almost surely converges to the true value i.e., $\hat{\lambda} \to \lambda$ as the window's area is increased. Table 3.1 consists of recorded estimates for a sample network realization and supports the fact that the estimation error reduces as the window size is made large. The theoretic MSE values are also provided.

TABLE 3.1

ESTIMATES OF λ FOR VARIOUS CIRCULAR WINDOW SIZES. TRUE VALUE: $\lambda = 1$

Window radius	25	50	75	100	200
Estimate of λ	0.9841	1.0339	1.0227	1.0190	1.0085
% Error	-1.59	3.39	2.27	1.9	0.85
MSE	5.1e-4	1.27e-4	5.7e-5	3.2e-5	8e-6

Once λ has been roughly estimated, confidence intervals can be established for it [14]. Crow et al. [30] provide approximate confidence intervals for λ, employing

the normal approximation and a continuity correction. If δ be the desired breadth of the confidence interval and ϵ the required confidence level, then

$$\delta\nu_2(W) \approx \left[\frac{z_{\epsilon/2}}{2} + \sqrt{1+\lambda\nu_2(W)}\right]^2 - \left[\frac{z_{\epsilon/2}}{2} - \sqrt{\lambda\nu_2(W)}\right]^2, \tag{3.10}$$

where $z_{\epsilon/2} = \mathrm{Q}^{-1}(\epsilon/2)$, and $\mathrm{Q}^{-1}(\cdot)$ is the inverse Q-function. From this, we can use the preliminary estimate of λ to obtain

$$\nu_2(W) \approx \frac{4z_{\epsilon/2}^2\lambda}{\delta^2}. \tag{3.11}$$

Accordingly, if one wishes to obtain an estimate of the intensity accurate to 2 decimal places ($\delta = 0.01$) with 99% confidence ($\epsilon = 0.01$), and a preliminary estimate of $\lambda = 1$, $\nu_2(W) = 266256$. A square of side about 500 units is needed to obtain an accurate estimate.

Alternatively, one can observe the process through N disjoint windows $W_1, \ldots, W_N$ and use the unbiased estimator

$$\hat{\lambda} = \frac{1}{n}\sum_{i=1}^{N}\frac{\Phi(W_i)}{\nu_2(W_i)}. \tag{3.12}$$

Since $\Phi(W_i)$ are independent random variables for each i, the following Crámer-Rao bound is established on the MSE.

$$\mathrm{MSE}(\hat{\lambda}) \geq \frac{\lambda}{\sum_{i=1}^{N}\nu_2(W_i)}. \tag{3.13}$$

Since this meets the regularity condition and is the minimum variance unbiased estimator, it is also the maximum-likelihood estimator. As a large number of windows are considered, the MSE vanishes. Also, if the window size is large, the MSE is nulled as seen before.

3.4.2 Estimation Based on Empty Quadrats

Here, the observation window W is partitioned into a large number of disjoint square subregions each of equal area a^2. The void probability for the PPP in each

of those small quadrats is equal to $p_0 = \exp(-\lambda a^2)$. Equating the fraction of empty quadrats to p_0, λ is estimated as

$$\hat{\lambda} = \ln(1/p_0)/a^2. \tag{3.14}$$

The estimates of the intensity for a sample realization of the PPP are shown in Table 3.2. To obtain these estimates, we generated a PPP with unit intensity on a 150×150 square window and used quadrats of size $a \times a$. The smaller a, the more accurate is the estimate, since it is based on more quadrats which permits better averaging. Note that this method can also be performed with subregions of equal area, that are not necessarily squares.

TABLE 3.2

ESTIMATES OF λ USING THE EMPTY QUADRATS METHOD. TRUE VALUE OF $\lambda = 1$

a	2	1	0.5	0.25
$\hat{\lambda}$	1.0366	1.0055	0.9979	0.9994
% Error	3.66	0.55	-0.21	-0.06

3.4.3 Estimation Based on Nearest Neighbor Distances

In certain situations, it might be possible to measure distances between nodes in the network. One such case is where the location of some nodes are known and these act as beacons assisting other nodes to estimate their locations. The knowledge of the nearest neighbor distances can be used to assist in estimating the network's intensity.

In a homogeneous Poisson network, it is well-known that the neighbor distances follow a generalized gamma distribution [31]. Accordingly, the density of the dis-

tance to the k^{th}-nearest neighbor for a planar network is given by

$$f(d_k = r; \lambda) = \exp(-\lambda\pi r^2)\frac{2(\lambda\pi r^2)^k}{r\Gamma(k)}, \quad k = 1, 2, \ldots. \tag{3.15}$$

The maximum-likelihood (ML) estimate of λ is obtained from here by setting [29]

$$\frac{\partial}{\partial\lambda} f(d_k = r; \lambda)|_{\lambda=\hat{\lambda}_{\text{ML}}} = 0,$$

which gives

$$\hat{\lambda}_{\text{ML}} = k/\pi r^2. \tag{3.16}$$

For a more accurate result, we can use N beacon nodes to make a N-sized vector measurement, resulting in the ML estimate

$$\hat{\lambda}_{\text{ML}} = \frac{Nk}{\pi \sum_{i=1}^{N} r_i^2}. \tag{3.17}$$

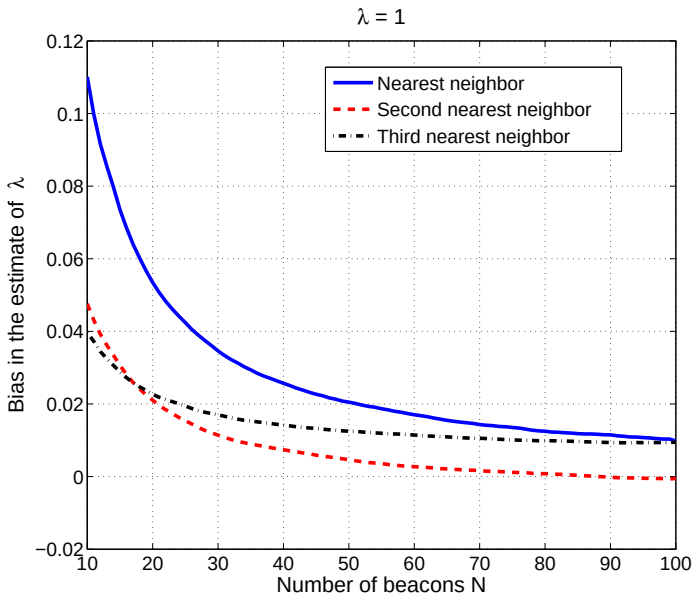

Figure 3.3. The bias in $\hat{\lambda}_{\text{ML}}$ for the k^{th} nearest neighbor measurements captured from N beacons for $k = 1, 2, 3$.

However, as Fig. 3.3 depicts, the ML estimate is biased. Moreover, the bias takes on negative values as well. The CRLB for an unbiased estimate of λ is given by the inverse of the Fisher information as

$$\begin{aligned} \text{CRLB} &= \frac{1}{\mathbb{E}_R\left[\frac{\partial^2}{\partial\lambda^2}\ln f(R;\lambda)\right]} \\ &= \frac{\lambda^2}{kN}. \end{aligned} \tag{3.18}$$

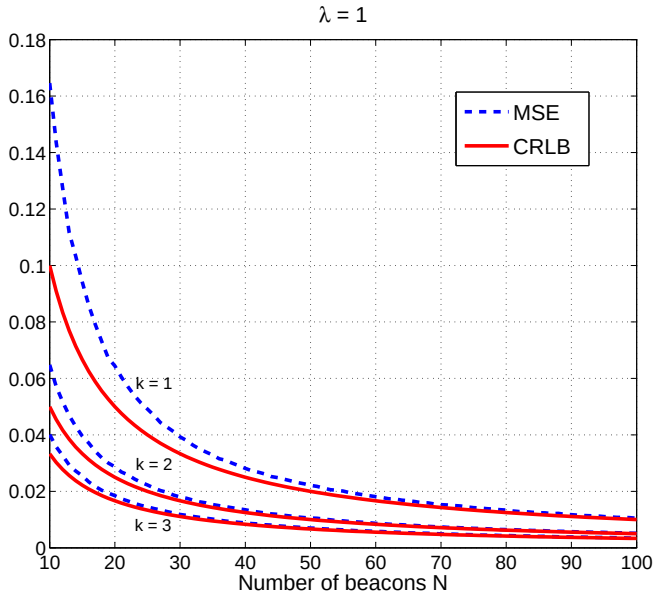

Figure 3.4. The MSE of $\hat{\lambda}$ against the CRLB for the k^{th} nearest neighbor measurements captured from N beacons for $k = 1, 2, 3$.

Fig. 3.4 plots the MSE and the CRLB for the estimates obtained from the first three neighbors' distance measurements. Though it is seen that the estimation error is lowered with farther neighbors, it is harder to make such measurements since it requires information to be relayed across more nodes.

3.5 Path Loss Exponent Estimation

This section describes three algorithms for PLE estimation and also provides simulation results on the estimation errors. Each method is based on a certain network characteristic namely the interference moments, the outage probabilities and the network's connectivity properties, respectively. The PLE estimation problem is essentially tackled by equating the practically measured values of these quantities to the theoretically established ones to obtain $\hat{\gamma}$. There is a caveat though, that needs to be addressed. In theory, we assume that we have access to a large number of realizations and usually derive results for an "average network", that is the one obtained by averaging over all possible realizations of the nodal distributions and the channel. However, the problem in practice is that we have only a single realization of the nodal distribution at hand. Fortunately, in the scenario where nodes are distributed as a homogeneous PPP, we can work around this issue by using its property of ergodicity. We now state the ergodic theorem for spatial processes that states that statistical averages of measurable functions may be replaced by spatial averages. Using this, we argue that a single realization of the network is sufficient for accurate estimation of the PLE.

Theorem 4. *(Ergodic Theorem [14, p. 172]) Let $T : X \to X$ be a measure preserving ergodic transformation on a measure space (X, Σ, ν) and consider a "well-behaved" function (more precisely, f must be L^1-integrable w.r.t the measure ν i.e., $f \in L^1(X, \Sigma, \nu)$). Define the "time-average" of f, $\hat{f}(x)$ as the average over iterations of T starting at some initial point x. Accordingly,*

$$\hat{f}(x) = \lim_{n\to\infty} \frac{1}{n} \sum_{k=0}^{n-1} f(T^k x), \tag{3.19}$$

where T^k is the k^{th} iterate of T. Likewise, the spatial average of f is defined as

$$\bar{f}(x) = \frac{1}{\nu(X)} \int f d\nu. \tag{3.20}$$

Assuming that $\nu(X)$ is nonzero and finite, $\hat{f}(x) = \bar{f}(x)$ almost everywhere.

The ergodic theorem states that for an ergodic endomorphism, the space and time averages are equal almost everywhere. Let T denote the transformation whose iterates result in different realizations of the PPP. Since the PPP is ergodic, T represents a measure-preserving ergodic transformation. Thus, while $\hat{f}(x)$ reflects the average of f over different realizations of the PPP at a single node, $\bar{f}(x)$ is equivalent to taking an average over different nodes in a single realization, and these two are equal almost everywhere. In conclusion, we remark that the estimation process can be performed in practice by looking only at a single realization of the network and taking the necessary measurements over several nodes.

3.5.1 Estimation Using the Moments of the Interference

A simple technique to infer the PLE γ uses the knowledge of the interference moments. Using the estimation value of the PLE and the predicted value of the intensity of the Poisson process (from the previous section), we can also infer the parameters p and m.

According to this method, nodes simply need to record the strength of the interference power that they observe. By the ergodic theorem, the mean and variance of the set of measurements at several different nodes match the theoretically determined values. We first state existing theoretic results and subsequently describe how the estimation can be performed in practice.

For the PPP network running the slotted ALOHA protocol, the n^{th} cumulants of the interference resulting from transmitters in an annulus of inner radius A and outer radius B around the receiver node are given as [32]

$$C_n = 2\pi\lambda p \mathbb{E}_G[G^n] \frac{B^{2-n\gamma} - A^{2-n\gamma}}{2 - n\gamma}. \tag{3.21}$$

In particular, we can let B to be large (considering the entire network) so that the

mean and variance of the interference are

$$\mu_I = C_1 = 2\pi\lambda p \frac{A^{2-\gamma}}{\gamma - 2} \tag{3.22}$$

and

$$\sigma_I^2 = C_2 = 2\pi\lambda p \left(1 + \frac{1}{m}\right) \frac{A^{2-2\gamma}}{2\gamma - 2}. \tag{3.23}$$

Note that if $A = 0$ and $\gamma > 2$ (a fair assumption in a wireless scenario), all the moments of the interference are infinite. However, in practice, nodal dimensions are finite and therefore, this singularity condition is not observed. Denote the minimum spacing between nodes (antennas) by a constant A_0, that is known. Thus, in reality, there can be no transmitters inside a disc of radius A_0 around any node. In other words, A_0 can be considered to be the guard zone radius.

The algorithm based on the interference moments works by matching the practical and theoretic values of the mean interference and is described as follows.

1) Consider an arbitrary node in the network and number it node 1. Record the value of the interference power (received power) at node 1, I_1.

2) Repeat the above method for the other nodes $(2, \ldots)$ recording values of interference powers $I_2, \ldots$ at the respective nodes. Eventually, the empirical mean interference $(1/N)\sum_{i=1}^{N} I_i$ converges for some node number N.

By the ergodic theorem, the observed mean value matches the one given by (3.22) with $A = A_0$. The value of γ can be estimated by using a look-up table and the known values of A_0, p and estimated intensity $\hat{\lambda}$.

Alternatively, we can use a "differential method" that is based on measurements taken for two different guard zone radii values. This algorithm assumes that each node has information on its location and creating guard zones is feasible. Basically, one needs to measure the mean interference values μ_I^1 and μ_I^2 for guard zone radii A_1 and A_2 respectively. Since these observed values of the mean interference match

the theoretic values closely, we obtain

$$\frac{\mu_I^1}{\mu_I^2} = \left(\frac{A_1}{A_2}\right)^{2-\gamma},$$

and an unbiased estimate of γ is

$$\hat{\gamma} = 2 - \frac{\ln(\mu_I^1/\mu_I^2)}{\ln(A_1/A_2)}. \tag{3.24}$$

The advantage of the differential method is that it does not require the knowledge of the ALOHA contention probability p or the intensity of the process.

Fig. 3.5 depicts a stem plot of the histogram of the estimated PLE values. The predicted values fit well into a Gaussian curve (solid line) with the same statistics as the estimates, meaning that the estimation error is approximately Gaussian in nature. The estimate of γ is also seen to closely match its true value of 4.

The estimate $\hat{\gamma}$ can be used along with $\hat{\lambda}$ to predict the value of the transmission probability p. Indeed, using (3.22), an estimate of the ALOHA contention parameter is obtained immediately as

$$\hat{p} = \frac{\mu_I^1(\hat{\gamma} - 2)}{2\pi\hat{\lambda}A_1^{2-\gamma}}. \tag{3.25}$$

Furthermore, an estimate of the fading parameter m is obtained by inverting (3.23) as

$$\hat{m} = \left(\frac{\sigma_I^2(\hat{\gamma} - 1)}{\pi\hat{\lambda}\hat{p}A_1^{2-2\hat{\gamma}}} - 1\right)^{-1}, \tag{3.26}$$

where σ_I^2 is the empirical variance of the interference for guard zone radius A_1.

For the case that the channels are Rayleigh-faded (exponential received powers), we formulate two other schemes for the estimation process. The first method concerns outage probabilities, while another technique makes use of the connectivity properties of the network.

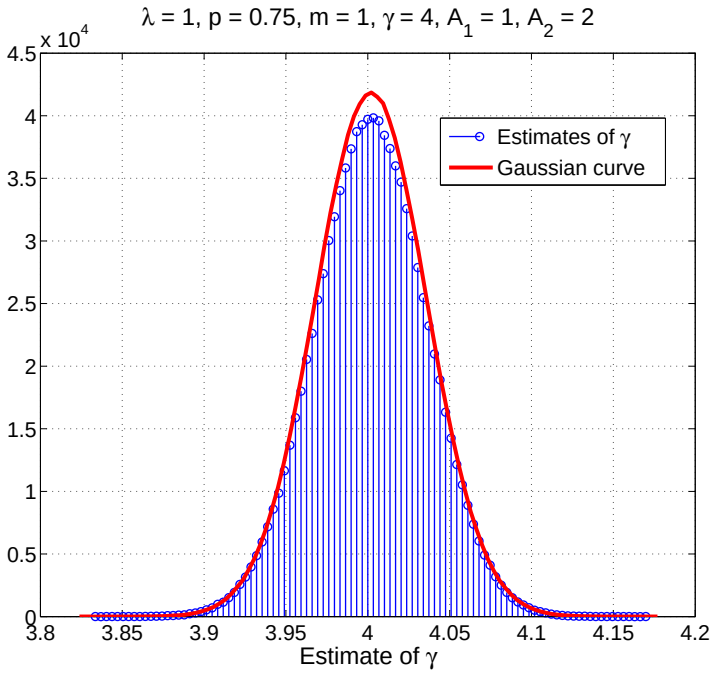

Figure 3.5. Histogram of $\hat{\gamma}$ for the estimation algorithm based on the interference moments. Error variance ≈ 0.0015.

3.5.2 Estimation Based on Outage Probabilities

In the estimation procedure using the moments of the interference, a suitable guard zone needs to be imposed around each receiver node. This might not be a practical/feasible solution, particularly in cases where there is no relative node location information available. When it is known that the channel fading is Rayleigh, the PLE can also be estimated using outage probabilities as discussed below. Similar to the previous algorithm, here too, we do not need an estimate of λ or the value of p. We first derive some theoretic results and latterly describe a practical scheme to guess γ.

By Slivnyak's theorem [14], the distribution of the PPP is unaffected by the addition of a point to the process but removing it from consideration. The intro-

duction of this point is useful in formalizing the notion of a "typical point" of the process. Given this, consider an arbitrary node in the network and in addition, place a transmitter at unit distance away from it[2]. Now, we shift the transmitter node to the origin and consider the outage probability for this typical node pair. Assume that noise and interference are independent of each other. The probability of success for this transceiver pair is given by

$$\begin{aligned} p_s &= \mathbb{E}_I^{!0}\left[\Pr(G > (N_0 + I)\Theta \mid I)\right] \\ &= \exp(-N_0\Theta)\mathbb{E}_I^{!0}\left[\exp\left(-I\Theta\right)\right] \\ &= \exp(-N_0\Theta)M_I\left(\Theta\right), \end{aligned} \tag{3.27}$$

where $M_I(s)$ is the MGF of the interference power I and $\mathbb{E}_I^{!0}$ denotes the expectation with respect to the reduced Palm measure [14]. It is basically the expectation conditioned on there being a point at the origin 0, but not including the point for calculation of the interference power. Using the closed-form expression for the MGF [32, Eqn. 20], we have for $\gamma > 2$,

$$p_s = c_1 \exp(-c_2), \tag{3.28}$$

where $c_1 = \exp(-N_0\Theta)$ and $c_2 = \lambda p\pi\Gamma\left(1 + 2/\gamma\right)\Gamma\left(1 - 2/\gamma\right)\Theta^{2/\gamma}$. The outage probability $1 - p_s$ is plotted versus γ in Fig. 3.6 for different values of threshold.

For the rest of this subsection, we assume that the system is interference-limited. In other words, $N_0 \ll I$ and therefore, $p_s \approx \exp(-c_2)$. We now describe a practical scheme to estimate γ. The idea behind this algorithm is to compute the SIR values at each node and use the empirical distribution to compute the success probability, which by the ergodic theorem, matches the theoretic value. It works as follows.

1) Consider an arbitrary node, call it the receiving node and place a transmitter at a unit distance away from it. The transmitter should not belong to the original

[2]The distance requirement is just a convenient assumption so that when the transceivers are unit distance apart, the PLE will not affect the received power strength

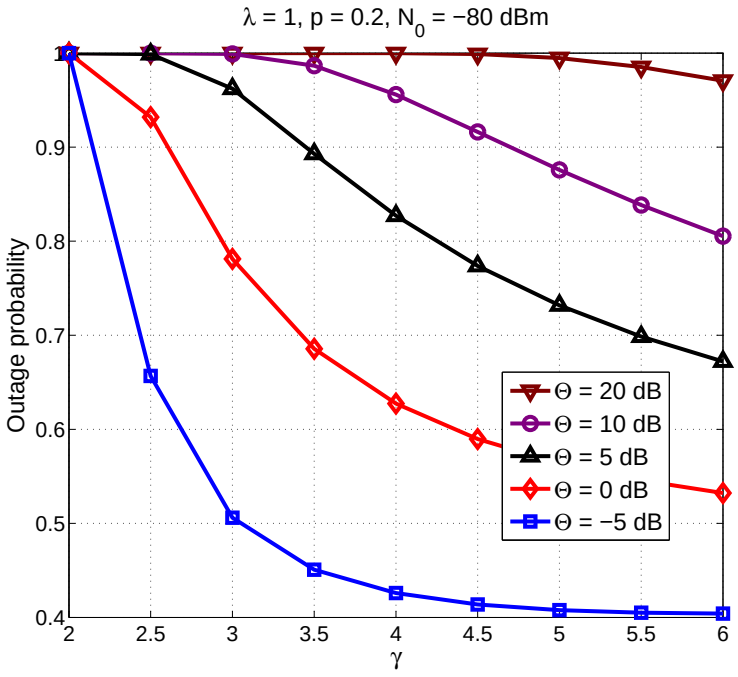

Figure 3.6. Theoretical values of the outage probabilities at different thresholds.

process. With a transmit power of unity, the received power due to that transmitter alone is exponential with unit mean. Measure the SIR at this receiver node.

2) Repeat for several nodes, thus obtaining a histogram of the measured SIR values. For any given value of Θ, the probability of success can be empirically determined from the histogram.

The success probability obtained thus matches the one given by (3.28). If it is possible to measure the value of p, a look-up table can be generated to estimate the PLE using the known value of p and an estimated intensity $\hat{\lambda}$.

If the density of the network or p is not accurately known, we can use a differential method to estimate γ. Accordingly, obtain histograms of the measured SINR for two different values of the threshold, say Θ_1 and Θ_2. Denote the empirical values of the success probabilities corresponding to the two values of Θ as p_s^1 and p_s^2.

Theoretically, we obtain

$$\frac{\ln(p_s^1)}{\ln(p_s^2)} = \frac{\ln(M_I(\Theta_1))}{\ln(M_I(\Theta_2))} = \left(\frac{\Theta_1}{\Theta_2}\right)^{2/\gamma},$$

and therefore an unbiased estimate of γ is

$$\hat{\gamma} = \frac{2\ln(\Theta_1/\Theta_2)}{\ln(\ln(p_s^1)/\ln(p_s^2))}. \tag{3.29}$$

Fig. 3.7 plots the histogram of the estimated PLE values when the true value is $\gamma = 4$. The estimation error fits well into a Gaussian curve for this scheme as well.

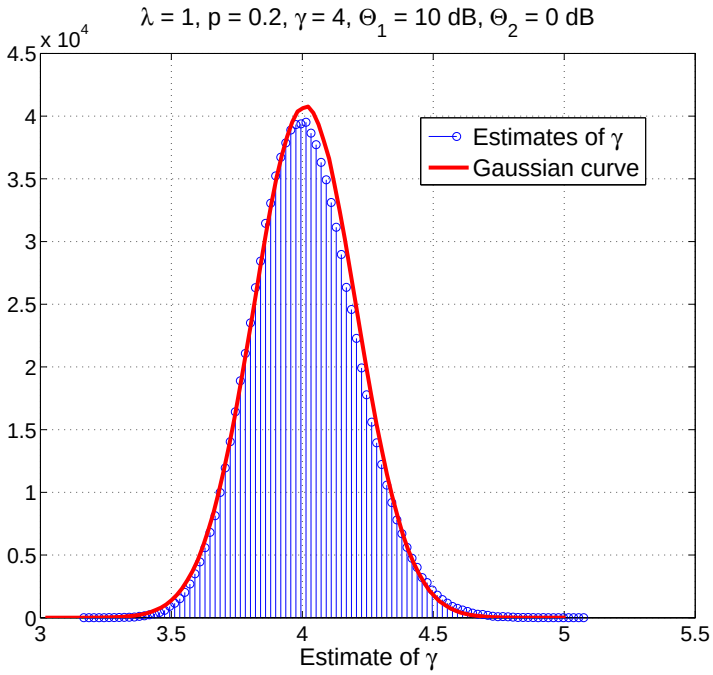

Figure 3.7. Histogram of $\hat{\gamma}$ for the method based on outage probabilities. Error variance ≈ 0.04.

We remark that it may not seem practical to place the transmitter for each receiver node where measurements are taken. Instead, nodes can equivalently assume the existence of a virtual transmitter and assume the signal power to be an expo-

nential random variable with unit mean. This way, they can simply measure the interference power alone and compute the SIR.

Error analysis when the fading distribution is not necessarily Rayleigh :

A critical assumption used for the estimation algorithm based on outage probabilities is that the fading component of the channel is Rayleigh distributed. It is interesting to see how much the Nakagami fading parameter m affects the estimation results, i.e., how large the error is in the case that the fading distribution is not actually Rayleigh, but assumed to be so. We now provide some empirical results to depict the behavior of the error when the true value of m is not unity.

Fig. 3.8 shows the CDF of the error for some values of m ranging from 0.5 to ∞. For a slight deviation of m from unity, the predicted values differ largely from the true value, particularly when the fading effect is stronger than Rayleigh fading ($0.5 \leq m < 1$). The dotted line for $m = 1$ shows that the error median in this case is 0. Moreover, since the error is roughly Gaussian distributed, we conclude that the estimate of γ is unbiased when the channel is indeed Rayleigh. We also observe that the error CDF converges as $m \to \infty$.

Fig. 3.9 plots the MSE, taken over several different network realizations versus m for different PLE values. Again, we observe that the performance of this algorithm depends critically on the fading parameter m especially at lower values, since a slight deviation of m from unity largely affects the estimation error.

As a supplement to the simulation results, we now analytically derive the outage probability when the fading component G is a general Nakagami-m distributed variable.

The pdf of the power fading variable is given by

$$p_G(g) = \frac{m^m}{\Gamma(m)} g^{m-1} \exp(-mg), \quad m \geq 0.5. \tag{3.30}$$

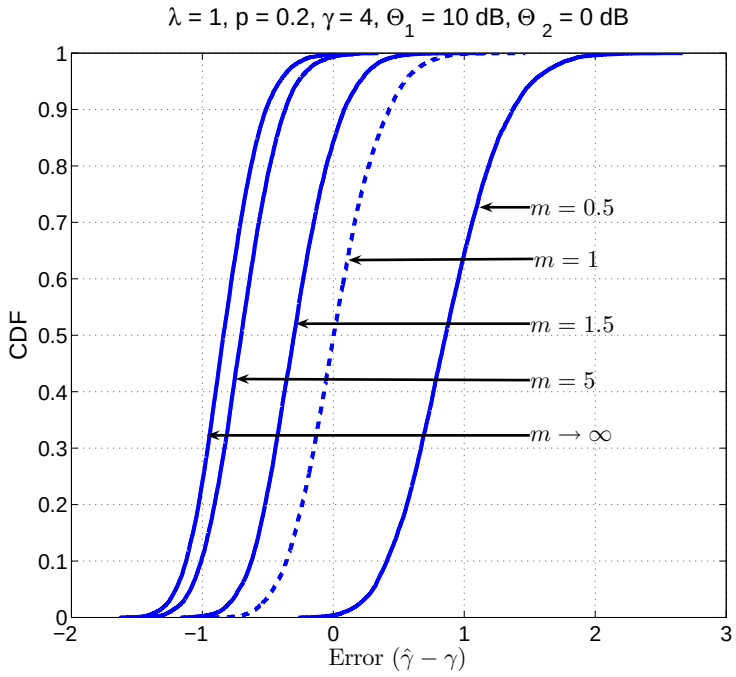

Figure 3.8. CDF of the error $\hat{\gamma} - \gamma$.

Using this, we have

$$\begin{aligned} p_s &= \mathbb{E}_I^{!0}\left[\Pr(G > I\Theta \mid I)\right] \\ &= \mathbb{E}_I^{!0}\left[\int_{I\Theta}^{\infty} \frac{m^m}{\Gamma(m)} g^{m-1}\exp(-mg)dg\right] \\ &= \frac{1}{\Gamma(m)}\int_0^{\infty} \Gamma(m, x\Theta m)P_I(x)dx, \end{aligned} \tag{3.31}$$

where $\Gamma(\cdot,\cdot)$ is the upper incomplete gamma function[3] and $P_I(x)$ denotes the pdf of the interference function.

The expressions can be further simplified when m is an integer. For $m \in \mathbb{Z}^+$, we

[3]Mathematica: Gamma[a,z]

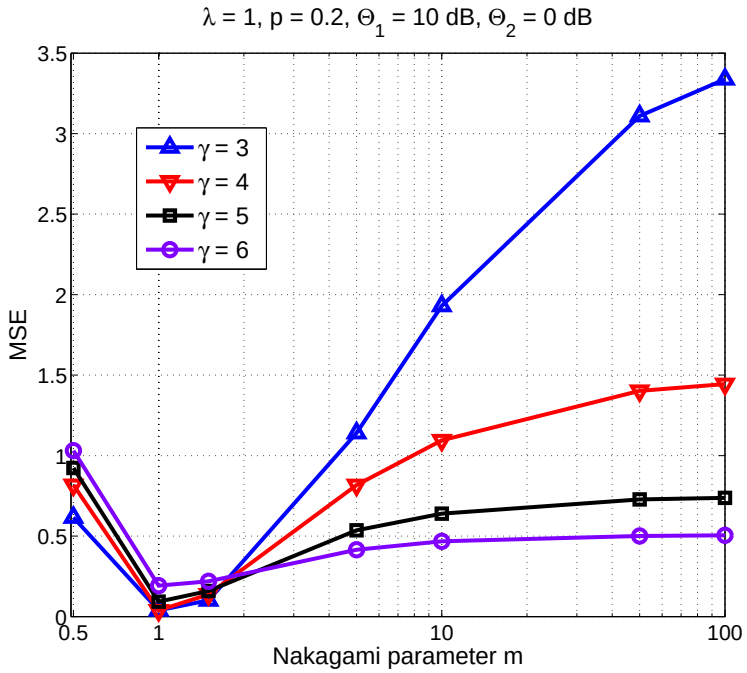

Figure 3.9. The value of the MSE versus m for different PLEs.

have

$$\begin{aligned} p_s &\overset{(a)}{=} \sum_{k=0}^{m-1} \frac{1}{k!} \int_0^{\infty} (x\Theta m)^k \exp(-x\Theta m) P_I(x) dx \\ &\overset{(b)}{=} \sum_{k=0}^{m-1} \frac{(-\Theta m)^k}{k!} \frac{d^k}{ds^k} M_I(s)|_{s=\Theta m}, \end{aligned} \tag{3.32}$$

where (a) is obtained from the series expansion of the upper incomplete gamma function and (b) from the definition of the MGF. We also have the following closed-form expression for the MGF [32, Eqn. 20]

$$M_I(s) = \exp(-\lambda p \pi \mathbb{E}_G[G^{2/\gamma}] \Gamma(1 - 2/\gamma) s^{2/\gamma}).$$

Using this, we get

$$p_s = \exp(-c_3) \sum_{k=0}^{m-1} \frac{c_3^k}{k!} \left(\frac{2}{\gamma}\right)^k, \tag{3.33}$$

where $c_3 = \lambda p \pi \mathbb{E}_G(G^{2/\gamma})\Gamma(1-2/\gamma)(\Theta m)^{2/\gamma}$. The outage probabilities at integer values of m for $\gamma > 2$ can be numerically evaluated from the above equation.

3.5.3 Estimation Based on the Cardinality of the Transmitting Set

In this subsection, we present a method to estimate the PLE based on the connectivity properties of the network. For any node, define its transmitting set as the group of transmitting nodes whom it receives a packet from, in a given time slot. More formally, for receiver y, transmitter node x is in its transmitting set if they are connected i.e., the SINR at y is greater than a certain threshold Θ. Note that this set changes from time slot to time slot. This algorithm is based on matching the theoretic and practical values of the mean number of elements in the transmitting set. Note that for $\Theta = 0$ dB, the condition for a transceiver pair to be connected is that the received signal strength is greater than the interference power. Thus, for $\Theta \geq 1$, the cardinality of the transmitting set can at most be one, and that transmitter is the one with the best channel to the receiver. The following proposition forms the basis of the estimation algorithm.

Proposition 5. *Under the conditions of Rayleigh fading and $N_0 \ll I$, the cardinality of the transmitting set is Poisson distributed with parameter* $(\Gamma(1+2/\gamma)\Gamma(1-2/\gamma)\Theta^{2/\gamma})^{-1}$.

Proof: Extending the procedure used for deriving (3.28), we see that the success probability for a transceiver pair at an arbitrary distance R units apart is

$$p_s(R) = c_1'(R)\exp(-c_2 R^2),$$

where $c_1'(R) = \exp(-N_0 R^\gamma \Theta)$. For $N_0 \ll I$, $p_s \approx \exp(-c_2 R^2)$. Now, we place an additional receiver node O at the origin (which does not affect the distribution of the PPP) and analyze the transmitting set for this "typical" node.

Consider a disc of radius a centered at the origin. Let E_i denote the event that the ith transmitter inside this disc is in O's transmitting set. For R uniformly

distributed in $[0, a]$, we have

$$\begin{aligned}\mathbb{P}(E_i) &= \mathbb{E}_R[p_s(R) \mid R] \\ &= \frac{2\pi}{\pi a^2}\int_0^a re^{-c_2 r^2}dr \\ &= \frac{1}{a^2 c_2}(1 - e^{-a^2 c_2}). \end{aligned} \tag{3.34}$$

Note that in any given time slot, the events E_i and E_j for arbitrary transmitters i and j are actually slightly correlated. This is because i acts as an interferer for j's signal and vice versa. We neglect this minor dependence and assume that the E_i's are independent events. Also, since $\mathbb{P}(E_i)$ is independent of i, we take $\mathbb{P}(E_i) = \mathbb{P}(E)$, $\forall i$, to simplify notation. Denote the mean number of transmitters in the disc of radius a by $N_a = \lambda p \pi a^2$. Then, the probability of having exactly k elements in the transmitting set T is calculated as

$$\begin{aligned}\mathbb{P}(N_T = k) &= \lim_{a\to\infty} \mathbb{E}_{N:N\geq k}\left[\binom{N}{k}\mathbb{P}(E)^k(1-\mathbb{P}(E))^{N-k}\right] \\ &= \lim_{a\to\infty}\sum_{n=k}^{\infty}\frac{e^{-N_a}N_a^n}{n!}\binom{n}{k}\mathbb{P}(E)^k(1-\mathbb{P}(E))^{n-k} \\ &\overset{(a)}{=} \lim_{a\to\infty}\frac{(\mathbb{P}(E)N_a)^k}{k!}\sum_{s=0}^{\infty}\frac{e^{-N_a}N_a^s}{s!}\cdot(1-\mathbb{P}(E))^s \\ &= \lim_{a\to\infty}\frac{(\mathbb{P}(E)N_a)^k}{k!}\exp(-N_a\mathbb{P}(E)) \\ &= \exp(-c_4)c_4^k/k!, \end{aligned} \tag{3.35}$$

where (a) is obtained on using the substitution $n-k = s$, and $c_4 = \lim_{a\to\infty} N_a\mathbb{P}(E) = 1/(\Gamma(1+2/\gamma)\Gamma(1-2/\gamma)\Theta^{2/\gamma})$. □

Therefore, the cardinality of the transmitting set, N_T, is distributed as a Poisson random variable with mean c_4, and is, surprisingly, independent of λ and p. Because of the homogeneity in the nodal arrangement, the size of each node's transmitting set obeys the same statistics. Fig. 3.10 plots the theoretic expected size of the transmitting set $\bar{N}_T$ for different threshold values at various PLE values.

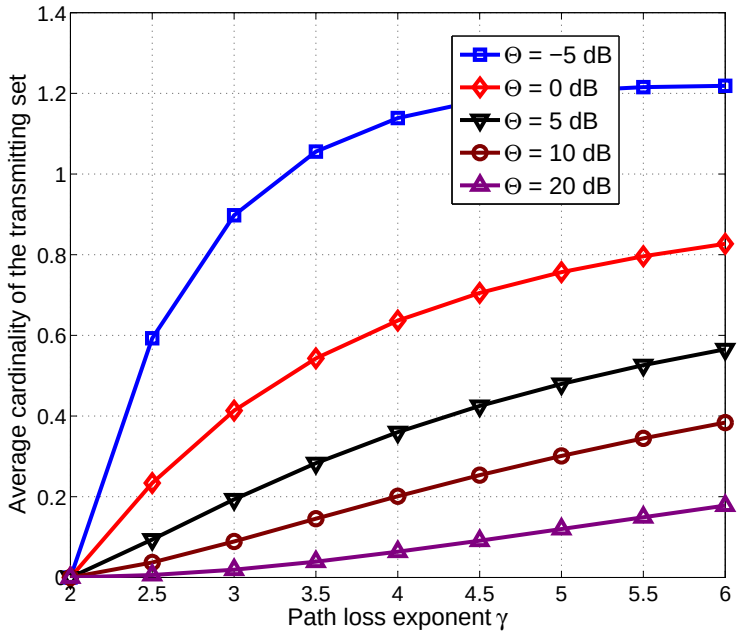

Figure 3.10. The mean number of elements in the transmitting set versus γ for different SIR threshold values.

Comparing the empirical mean cardinality of the transmitting set to c_4, γ can be estimated using a look-up table. Alternatively, we may use a differential method where we measure the mean cardinalities of the transmitting sets for two different values of Θ, Θ_1 and Θ_2. Denote the mean transmitting set sizes corresponding to the two values of Θ as $\bar{N}_T^1$ and $\bar{N}_T^2$. Theoretically, we obtain

$$\frac{\bar{N}_T^1}{\bar{N}_T^2} = \left(\frac{\Theta_2}{\Theta_1}\right)^{2/\gamma},$$

giving us an unbiased estimate as

$$\hat{\gamma} = \frac{2\ln(\Theta_2/\Theta_1)}{\ln(\bar{N}_T^1/\bar{N}_T^2)}. \tag{3.36}$$

Fig. 3.11 plots the histogram of the estimated PLE values when the actual value is $\gamma = 4$. The estimation error for this scheme also seems approximately Gaussian.

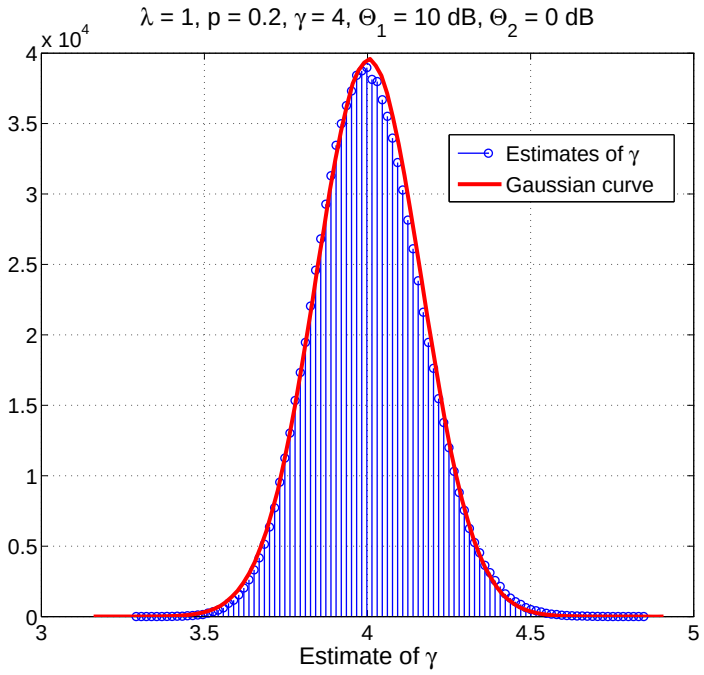

Figure 3.11. Histogram of $\hat{\gamma}$ for the estimation algorithm based on the cardinality of the transmitting set. Error variance ≈ 0.03.

We now analytically evaluate the Crámer-Rao lower bound for an unbiased estimate of N_T. From (3.35), we have

$$\ln f(N_T = k; \gamma) = -c_4 + k \ln(c_4) - \ln(k!) \tag{3.37}$$

The Fisher information for an unbiased estimate of γ is then given by

$$\begin{aligned} J(\gamma) &= \mathbb{E}_{N_T}\left[-\frac{\partial^2}{\partial \gamma^2} \ln f(N_T;\gamma)\right] = \frac{1}{c_4}\left(\frac{\partial c_4}{\partial \gamma}\right)^2 \\ &= \frac{4\left[\psi(1-\frac{2}{\gamma}) - \psi(1+\frac{2}{\gamma}) - \ln(\Theta)\right]^2}{\gamma^4 \Gamma(1+\frac{2}{\gamma})\Gamma(1-\frac{2}{\gamma})\Theta^{\frac{2}{\gamma}}}, \end{aligned} \tag{3.38}$$

where $\psi(x)$ represents the digamma function[4] and has the integral representation

$$\psi(x) = \int_0^\infty \left(\frac{e^{-t}}{t} - \frac{e^{-xt}}{1-e^{-t}}\right) dt.$$

[4]Mathematica: PolyGamma[x]

We have CRLB $= 1/J(\gamma)$.

Error analysis when the fading distribution is not necessarily Rayleigh :

The method based on the cardinality of the transmitting set assumes that channel is Rayleigh-faded. It is interesting to see how large the error is when the true value of m is not 1. We now derive some analytical results showing the dependence of the algorithm on the fading parameter m. Specifically, we determine the distribution of N_T for integer values of m and comment on its effect on the estimation algorithm.

When G is a Nakagami-m distributed variable, we can generalize (3.33) to obtain the success probability for a transceiver pair at an arbitrary distance R units apart as

$$p_s(R) = \sum_{k=0}^{m-1} \frac{\exp(-c_3 R^2)\,(c_3 R^2)^k}{k!} \left(\frac{2}{\gamma}\right)^k, \quad m \in \mathbb{Z}^+. \tag{3.39}$$

Using this, we obtain

$$\begin{aligned}
\mathbb{P}(E) &= \mathbb{E}_R[p_s(R) \mid R] \\
&= \frac{2\pi}{\pi a^2} \int_0^a \sum_{k=0}^{m-1} \frac{\exp(-c_3 r^2) r^{2k}}{k!} \left(\frac{2c_3}{\gamma}\right)^k r dr \\
&= \frac{1}{a^2} \sum_{k=0}^{m-1} \left(\frac{2c_3}{\gamma}\right)^k \int_0^a \frac{\exp(-c_3 r^2)}{k!} r^{2k} 2r dr \\
&\overset{(a)}{=} \frac{1}{a^2 c_3} \sum_{k=0}^{m-1} \left(\frac{2}{\gamma}\right)^k \frac{1}{k!} \int_0^{c_3 a^2} t^k \exp(-t) dt \\
&\overset{(b)}{=} \frac{1}{a^2 c_3} \sum_{k=0}^{m-1} \left(\frac{2}{\gamma}\right)^k \frac{1}{k!} \left(1 - \Gamma(k+1, c_3 a^2)\right),
\end{aligned} \tag{3.40}$$

where (a) is obtained by a simple change of variables ($t = c_3 r^2$) and (b) using the definition of the incomplete gamma function. Following the steps used in the derivation of (3.35), the cardinality of the transmitting set is seen to be Poisson

distributed with mean c_5, where

$$\begin{aligned} c_5 &= \lim_{a\to\infty} N_a \mathbb{P}(E) \\ &\overset{(a)}{=} \frac{\lambda p \pi}{c_3} \sum_{k=0}^{m-1} \left(\frac{2}{\gamma}\right)^k \\ &= \frac{\lambda p \pi}{c_3} \frac{1-\left(\frac{2}{\gamma}\right)^m}{1-\frac{2}{\gamma}} \\ &\overset{(b)}{=} \frac{\Gamma(m)\left(1-\left(\frac{2}{\gamma}\right)^m\right)}{\Gamma(m+\frac{2}{\gamma})\Gamma(2-\frac{2}{\gamma})\Theta^{2/\gamma}}. \end{aligned} \tag{3.41}$$

Here, (a) is obtained using the fact that $\lim_{z\to\infty} \Gamma(a,z) = \Gamma(a)$ and (b) using the definition of c_3 and [15, Eqn. 17]

$$\mathbb{E}[G^{2/\gamma}] = \frac{\Gamma(m+2/\gamma)}{\Gamma(m)m^{2/\gamma}}.$$

The analytical value of the mean cardinality of the transmitting set when $m \in \mathbb{Z}^+$ is plotted in Fig. 3.12 for two different thresholds.

From (3.41), we see that $\bar{N}_T$ is inversely proportional to $\Theta^{2/\gamma}$. Therefore, if we use a differential method to estimate γ, we still obtain

$$\frac{\bar{N}_T^1}{\bar{N}_T^2} = \left(\frac{\Theta_2}{\Theta_1}\right)^{2/\gamma}.$$

Remarkably, when m is a positive integer, it has no effect on the performance of the algorithm. Based on this observation, we surmise that the behavior of the error is independent of m, even when $m \in \mathbb{R}$. Fig. 3.13 plots the empirical MSE for the differential method, taken over several different network realizations versus m for various PLE values. As expected, the MSE is insensitive to the fading parameter.

3.6 Comparison of the Algorithms

In this section, we compare the features of the three algorithms for PLE estimation described in the earlier section. A common characteristic of all the algorithms

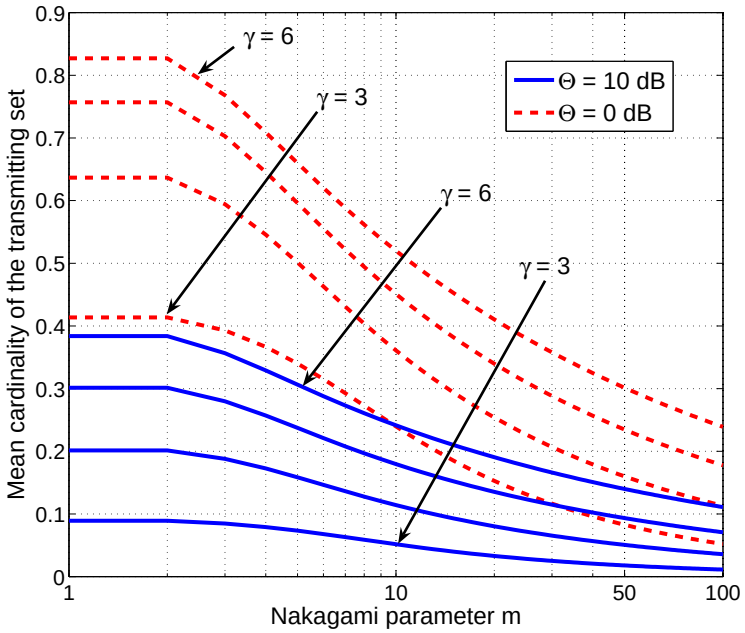

Figure 3.12. The expected cardinality of the transmitting set for various values of γ.

are that the estimation errors are (roughly) Gaussian, since the histogram of the errors fit well into normal distribution curves. Furthermore, the differential algorithms are seen to be accurate and do not require estimates of λ or the contention probability p.

1) The method that predicts γ using the knowledge of the interference moments can also be used to estimate p and m. It is seen to work well for a wide range of system parameters and importantly is accurate independent of the value of m. Though it is fairly simple in principle, it invokes a scheduling procedure for taking measurements, since all the nodes inside the guard zone are required to stop transmitting.

2) The scheme that estimates γ upon calculating outage probabilities does not

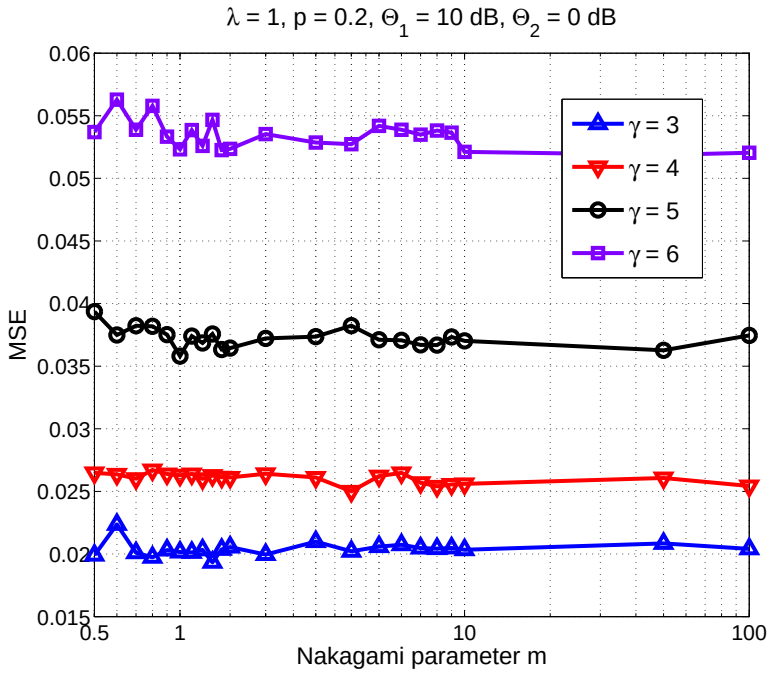

Figure 3.13. The value of the MSE versus m for different PLEs.

need a guard zone to be imposed, but requires a transmitter that originally did not belong to the process to be placed at unit distance from the receiver. Moreover, it is formalized only for the Rayleigh fading case ($m = 1$). The error is seen to be high when fading is severe (values of m lower than 1), and more so when the PLE is high. Also, this algorithm is convenient to use only when the network is interference-limited, i.e., the noise level is considerably lower than the interference power.

3) The algorithm based on the connectivity properties of the PPP does not need any node location information or the imposition of a guard zone around the nodes. Furthermore, it is robust in the sense that it performs independently of the value of the fading parameter m. Like the previous algorithm, it is, however, based on the condition that the system is interference-limited.

We now address a couple of performance issues related to the rate of convergence of the algorithms. First, the success of these methods is critically determined by the number of survey points N to be taken. A small value of N will result in low accuracy while a large value of N will result in an expensive survey process with many of the survey points giving little benefit. The second aspect is related to centralized versus distributed information processing. Specifically, the efficiency of these techniques relies on how the nodes that take measurements are chosen. Consider the two extreme cases where nodes $1, 2, \ldots N$ can be chosen in a random fashion or as subsequent nearest neighbors. In the latter method, the first node relays its measurement information to its nearest neighbor which then passes this on along with its own measured value, to its nearest neighbor other than the first node, and information is propagated in this manner. If nodes are chosen this way in a local fashion, the measurements will be correlated and the algorithm takes a long time to converge. On the other hand, choosing nodes randomly may result in choosing nodes sufficiently far apart but will also incur a lot of overhead when information needs to be exchanged between nodes or relayed to a central server or a fusion center.

Fig. 3.14 compares the performance of the three algorithms. Here, R refers to the centralized computing scheme where measurements are taken at randomly picked nodes and relayed to the central server, while NN refers to the distributed algorithm where measurements are passed over to subsequent nearest neighbors. From the plot, we see that the algorithm based on the interference moments clearly has the lowest MSE. Also, for the first two schemes, choosing randomly located nodes for measurements leads to a much faster convergence than when choosing subsequent nearest neighbors. However, for the method based on the cardinality of the transmitting set, the order in which nodes are picked does not have a huge

impact on its convergence rate.

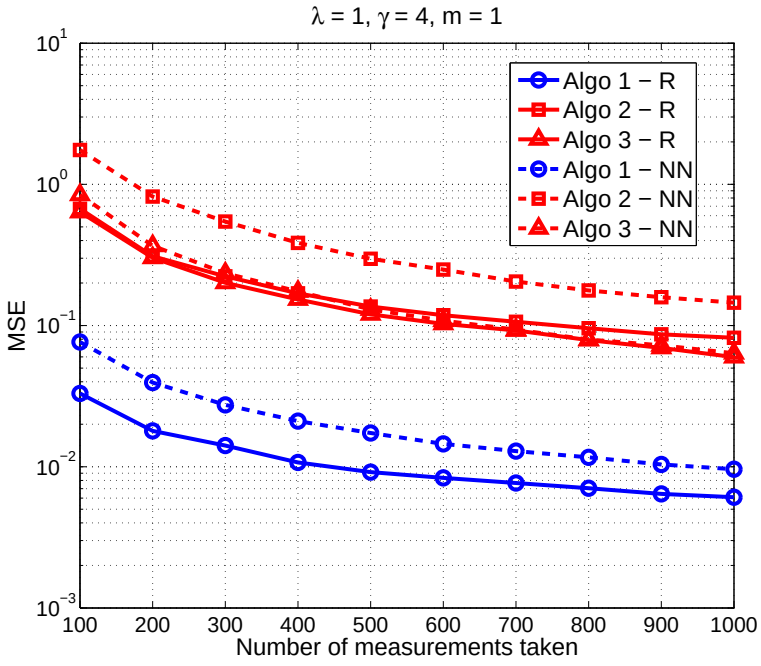

Figure 3.14. Comparison of the MSE performance of the three algorithms.

3.7 Chapter Summary

In wireless systems, the value of the PLE is critical but not known a priori, thus an accurate estimate is essential for the analysis and design of systems. We offer a fresh look at the issue of PLE estimation in a large wireless network, by taking into account Nakagami-m fading, the underlying node distribution and the network interference. Nodes are assumed to be arranged as a homogeneous PPP on the plane and the channel access scheme is slotted ALOHA. For such a system, this chapter describes three separate algorithms for PLE estimation. Simulation results are provided to demonstrate their performance and quantify the estimation errors. For each of the algorithms, we find that the estimation error is approximately

Gaussian. Comparing the algorithms, we see that the one that is based on the interference moments performs the best in terms of minimizing the MSE. We also provide methods to infer the intensity of the PPP and evaluate Crámer-Rao lower bounds on the MSE.

CHAPTER 4

SUMMARY AND CONCLUDING REMARKS

This thesis provides an analytical characterization of the interference in a wireless network with uniformly randomly distributed nodes. Applications include evaluating the network outage performance and estimating the path loss exponent of the channel, based on the properties of the interference.

It is a fact that taking interference into account for modeling wireless networks often makes the analysis intractable. It is for this reason that the modeling of interference has been studied for very few cases of the nodal distribution such as the PPP and the Poisson clustered process. In this work, we characterize the interference in a network where the nodes are distributed as a BPP. Based on the shot noise framework, a closed-form analytical expression for the MGF of the interference is obtained. We also study the outage performance of the network and conclude that using the Poisson network model in analyses provides an overly optimistic estimate of the network's performance when the number of interferers is small and the threshold Θ is high.

As an important application, we offer a novel look at the issue of PLE estimation in a large wireless network, by taking into account Nakagami-m fading, the PPP model and the network interference. In wireless systems, the value of the PLE is often not known a priori and thus an accurate estimate is crucial for the analysis and design of systems. The thesis describes three algorithms for path loss exponent

estimation, each based on a different network characteristic. Simulation results are provided to demonstrate their performance and quantify the estimation errors. Comparing the algorithms, we see that the one that is based on the interference moments performs the best in terms of minimizing the MSE.

Finally, we remark that in reality, the PLE value changes depending on the terrain category and the environmental conditions, and hence cannot be assumed to be a constant over the entire network. However, our algorithms are still useful since they can be used for obtaining local estimates, based on measurements taken over neighborhoods. For cases where the channel behavior is different for different regions of the network, it can be divided into sub-areas with constant γ that are analyzed separately.

BIBLIOGRAPHY

[1] I. F Akyildiz, W. Su, Y. Sankarasubramaniam and E. Cayirci, "A Survey on Sensor Networks," *IEEE Communications Magazine*, Vol. 40, Iss. 8, pp. 102-114, Aug. 2002.

[2] J. Ilow and D. Hatzinakos, "Analytic Alpha-Stable Noise Modeling in a Poisson Field of Interferers or Scatterers," *IEEE Transactions on Signal Processing*, Vol. 46, No. 6, pp. 1601-1611, June 1998.

[3] J. Venkataraman, M. Haenggi and O. Collins, "Shot Noise Models for Outage and Throughput Analyses in Wireless Ad Hoc Networks," *Military Communications Conference* (MILCOM'06), Washington DC, Oct. 2006.

[4] J. Venkataraman and M. Haenggi, "Optimizing the Throughput in Random Wireless Ad Hoc Networks," *42nd Annual Allerton Conference on Communication, Control, and Computing*, Oct. 2004.

[5] E. S. Sousa and J. A. Silvester, "Optimum Transmission Ranges in a Direct-Sequence Spread Spectrum Multihop Packet Radio Network," *IEEE Journal Selected Areas in Communucations*, Vol. 8, No. 4, pp. 762-771, Jun. 1990.

[6] M. Souryal, B. Vojcic and R. Pickholtz, "Ad Hoc Multihop CDMA networks with Route Diversity in a Rayleigh Fading Channel," *Proc. IEEE MILCOM*, Vol. 2, pp. 1003-1007, Oct. 2001.

[7] R. Mathar and J. Mattfeldt, "On the Distribution of Cumulated Interference Power in Rayleigh Fading Channels," *Wireless Networks*, Vol. 1, pp. 31-36, Feb. 1995.

[8] F. Baccelli, B. Błaszczyszyn and P. Mühlethaler, "An Aloha Protocol for Multihop Mobile Wireless Networks," *IEEE Transactions on Information Theory*, Vol. 52, No. 2, pp. 421-436, Feb. 2006.

[9] S. Weber, X. Yang, J. G. Andrews, and G. de Veciana, "Transmission Capacity of Wireless Ad Hoc Networks with Outage Constraints," *IEEE Transactions on Information Theory*, Vol. 51, pp. 4091-4102, Dec. 2005.

[10] X. Liu and M. Haenggi, "Throughput Analysis of Fading Sensor Networks with Regular and Random Topologies," *EURASIP Journal on Wireless Communications and Networking, Special Issue on Wireless Sensor Networks*, Vol. 2005, No. 4, pp. 554-564, Aug. 2005.

[11] M. Haenggi, "Outage and Throughput Bounds for Stochastic Wireless Networks," *IEEE International Symposium on Information Theory*, Sept. 2005.

[12] K. Hong and Y. Hua, "Throughput Analysis of Large Wireless Networks with Regular Topologies," *EURASIP Journal on Wireless Communications and Networking*, Vol. 2007, No. 1, pp. 3-13, Jan. 2007.

[13] R. Ganti and M. Haenggi, "Interference and Outage in Clustered Wireless Ad Hoc Networks," submitted to *IEEE Transactions on Information Theory*. Available at `http://arxiv.org/pdf/0706.2434.pdf`.

[14] D. Stoyan, W. S. Kendall and J. Mecke, "Stochastic Geometry and its Applications," Wiley & Sons, 1978.

[15] M. Nakagami, *The m-distribution : A General Formula for Intensity Distribution of Rapid Fading,* in W. G. Hoffman, "Statistical Methods in Radiowave Propagation", Pergamon Press, Oxford, U. K., 1960.

[16] A. Ephremides, "Energy concerns in wireless networks," *IEEE Wireless Communications*, Vol. 9, pp. 48-59, Aug. 2002.

[17] S. B. Lowen and M. C. Teich, "Power-Law Shot Noise," *IEEE Transactions on Information Theory*, Vol. 36, No. 6, pp. 1302-1318, Nov. 1990.

[18] G. Samorodnitsky and M. S. Taqqu, "Stable Non-Gaussian Random Processes: Stochastic Models with Infinite Variance," Chapman and Hall, 1994.

[19] P. J. Smith, "A Recursive Formulation of the Old Problem of Obtaining Moments from Cumulants and Vice Versa," *The American Statistician*, Vol. 49, No. 2, pp. 217-218, May 1995.

[20] E. Lukacs, "Applications of Faà di-Bruno's Formula in Mathematical Statistics," *The American Mathematical Monthly*, Vol. 62, No. 5, pp. 340-348, May 1955.

[21] A. Hasan and J. G. Andrews, "The Guard Zone in Wireless Ad Hoc Networks," *IEEE Trans. on Wireless Communications*, Vol. 6, No. 3, pp. 897-906, Mar. 2007.

[22] W. C. Jakes, "Microwave Mobile Communications," Wiley-IEEE Press, May 1994.

[23] A. Savvides, W. L. Garber, R. L. Moses and M. B. Srivastava, "An Analysis of Error Inducing Parameters in Multihop Sensor Node Localization," *IEEE Transactions on Mobile Computing*, Vol. 4, No. 6, pp. 567-577, Nov./Dec. 2005.

[24] N. Patwari, I. Hero, A. O. M. Perkins, N. Correal, and R. ODea, "Relative Location Estimation in Wireless Sensor Networks," *IEEE Transactions on Signal Processing*, Vol. 51, No. 8, pp. 2137-2148, Aug. 2003.

[25] A. Özgür, O. Lévêque and D. Tse, "Hierarchical Cooperation Achieves Optimal Capacity Scaling in Ad Hoc Networks," *IEEE Transactions on Information Theory*, Vol. 53, No. 10, pp. 3549-3572, Oct. 2007.

[26] M. Sikora, J. N. Laneman, M. Haenggi, D. J. Costello, Jr., and T. E. Fuja, "Bandwidth- and Power-Efficient Routing in Linear Wireless Networks," *IEEE Transactions on Information Theory*, Vol. 52, No. 6, pp. 2624-2633, June 2006.

[27] M. Haenggi, "On Routing in Random Rayleigh Fading Networks," *IEEE Transactions on Wireless Communications*, Vol. 4, No. 4, pp. 1553-1562, July 2005.

[28] G. Mao, B. D. O. Anderson and B. Fidan, "Path Loss Exponent Estimation for Wireless Sensor Network Localization," *Computer Networks*, Vol. 51, Iss. 10, pp. 2467-2483, July 2007.

[29] S. M. Kay, "Fundamentals of Statistical Signal Processing, Volume I: Estimation Theory," Prentice Hall, Mar. 1993.

[30] Edwin L. Crow; Robert S. Gardner, "Confidence Intervals for the Expectation of a Poisson Variable," *Biometrika*, Vol. 46, No. 3/4, pp. 441-453, Dec. 1959.

[31] M. Haenggi, "On Distances in Uniformly Random Networks," *IEEE Transactions on Information Theory*, vol. 51, pp. 3584-3586, Oct. 2005.

[32] S. Srinivasa and M. Haenggi, "Modeling Interference in Finite Uniformly Random Networks," *International Workshop on Information Theory for Sensor Networks (WITS '07)*, Santa Fe, June 2007.